

# A Fast Sampling Method of Exploring Graphlet Degrees of Large Directed and Undirected Graphs

Pinghui Wang<sup>1</sup>, Xiangliang Zhang<sup>2</sup>, Zhenguo Li<sup>3</sup>, Jiefeng Cheng<sup>3</sup>,  
John C.S. Lui<sup>4</sup>, Don Towsley<sup>5</sup>, Junzhou Zhao<sup>4</sup>, Jing Tao<sup>1</sup>, and Xiaohong Guan<sup>1,6</sup>

<sup>1</sup>MOE Key Laboratory for Intelligent Networks and Network Security, Xi'an Jiaotong University, China

<sup>2</sup>King Abdullah University of Science and Technology, Thuwal, SA

<sup>3</sup>Huawei Noah's Ark Lab, Hong Kong

<sup>4</sup>Department of Computer Science and Engineering, The Chinese University of Hong Kong, Hong Kong

<sup>5</sup>Department of Computer Science, University of Massachusetts Amherst, MA, USA

<sup>6</sup>Department of Automation and NLIST Lab, Tsinghua University, Beijing, China  
{phwang, jtao, jzzhao, xhguan}@sei.xjtu.edu.cn, xiangliang.zhang@kaust.edu.sa,  
{li.zhenguo, cheng.jiefeng}@huawei.com, cslui@cse.cuhk.edu.hk, towsley@cs.umass.edu

## ABSTRACT

Exploring small connected and induced subgraph patterns (CIS patterns, or graphlets) has recently attracted considerable attention. Despite recent efforts on computing the number of instances a specific graphlet appears in a large graph (i.e., the total number of CISes isomorphic to the graphlet), little attention has been paid to characterizing a node's graphlet degree, i.e., the number of CISes isomorphic to the graphlet that include the node, which is an important metric for analyzing complex networks such as social and biological networks. Similar to global graphlet counting, it is challenging to compute node graphlet degrees for a large graph due to the combinatorial nature of the problem. Unfortunately, previous methods of computing global graphlet counts are not suited to solve this problem. In this paper we propose sampling methods to estimate node graphlet degrees for undirected and directed graphs, and analyze the error of our estimates. To the best of our knowledge, we are the first to study this problem and give a fast scalable solution. We conduct experiments on a variety of real-world datasets that demonstrate that our methods accurately and efficiently estimate node graphlet degrees for graphs with millions of edges.

## 1. INTRODUCTION

Exploring connected and induced subgraph (CIS) patterns (i.e., motifs, also known as graphlets) in a graph is important for understanding and exploring networks such as online social networks (OSNs) and computer networks. As shown in Fig. 1, there is one 2-node undirected graphlet  $G_0$ , two 3-node undirected graphlets  $G_1$  and  $G_2$ , six 4-node undirected graphlets  $G_3, \dots, G_8$ , and thirteen 3-node directed graphlets  $G_1^{(3d)}, \dots, G_{13}^{(3d)}$ , which are widely used for characterizing networks' local connection patterns. However, nodes may occupy very different positions in the same graphlet. For example, the three leaf nodes (in black) of  $G_4$  in Fig. 1 are symmetric, so their positions belong to the same class. The other

node (in white) of  $G_4$  behaves more like a hub. According to the positions that nodes of a graphlet occupies, Przulj et al. [1] group the graphlet's nodes into one or more different automorphism *orbits*<sup>1</sup> (i.e., position classes). They observe that a node's graphlet orbit degree vector, or graphlet orbit degree signature, which counts the number of CISes that touch the node at a particular orbit, is a useful metric for representing the node's topology features. In fact, the graphlet orbit degree signature has been successfully used for protein function prediction [2] and cancer gene identification [3] by identifying groups (or clusters) of topologically similar nodes in biological networks. In addition to biological networks, graphlet orbit degree is also used for link prediction [4] and node classification [5] in online social networks, and hyponym relation extraction from Wikipedia hyperlinks [6].

However, it is computationally intensive to enumerate and compute graphlet orbit degrees for large graphs due to the combinatorial explosion of the problem. To solve this challenge, approximate methods such as sampling could be used in place of the brute-force enumeration approach. Despite recent progress in counting specific graphlets such as triangles [7–10] and 4-node motifs [11] that appear in a large graph, little attention has been given to developing fast tools for computing graphlet orbit degrees. Existing methods of estimating global graphlet counts are customized to sample all CISes in a large graph, but not tailored to meet the need of sampling CISes that include a **given node**.

To solve this problem, we propose a new method to estimate graphlet orbit degrees and to detect orbits with the largest graphlet orbit degrees for large graphs. The overview of our method is shown in Fig. 2. Our contributions are summarized as:

1) We propose a series of methods: Randgraf-3-1, Randgraf-3-2, Randgraf-4-1, Randgraf-4-2, Randgraf-4-3, and Randgraf-4-4 for randomly sampling 3 and 4-node CISes that include a given node.

2) Based on the series of sampling methods, we design scalable and computationally efficient methods, SAND and SAND-3D, to estimate graphlet orbit degrees for undirected and directed graphs respectively, and we also derive expressions for the variances of our estimates, which is of great value in practice since the variances can be used to bound the estimates' errors and determine the smallest necessary sampling budget for a desired accuracy.

3) We conduct experiments on a variety of publicly available datasets. Our experimental results show that SAND and SAND-

<sup>1</sup>The values of orbit IDs in Fig. 1 have no specific meaning. We set the values of orbit IDs same as [1].

Permission to make digital or hard copies of all or part of this work for personal or classroom use is granted without fee provided that copies are not made or distributed for profit or commercial advantage and that copies bear this notice and the full citation on the first page. Copyrights for components of this work owned by others than ACM must be honored. Abstracting with credit is permitted. To copy otherwise, or republish, to post on servers or to redistribute to lists, requires prior specific permission and/or a fee. Request permissions from permissions@acm.org.

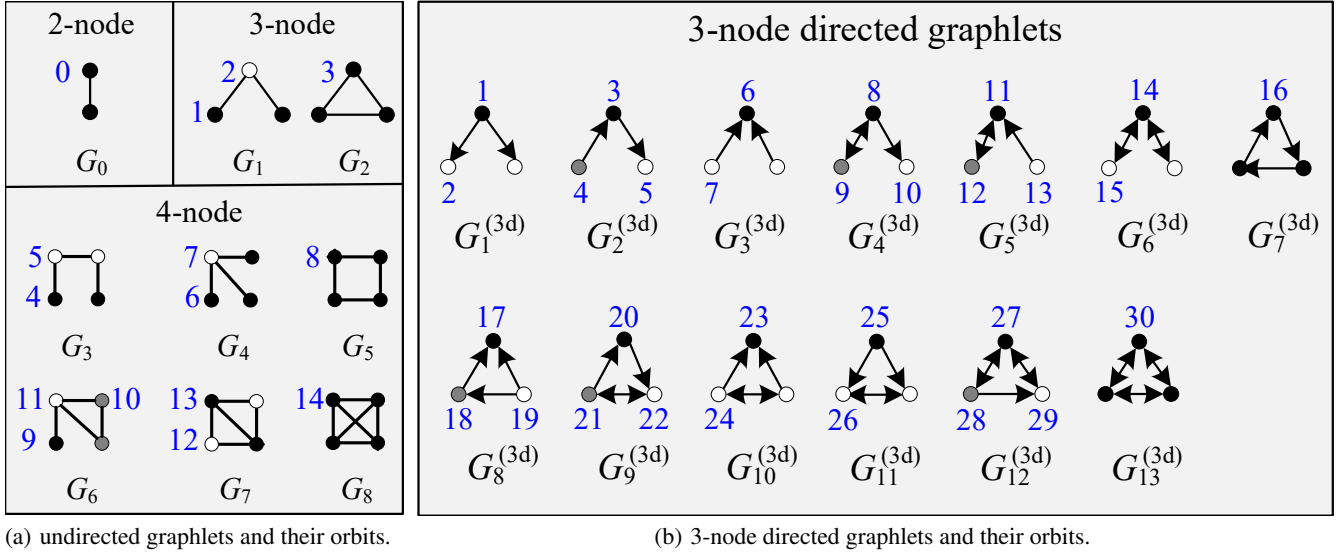


**Figure 1: Graphlets and their automorphism orbits studied in this paper.** Numbers in blue are orbit IDs. There is one 2-node undirected graphlet  $G_0$ , two 3-node undirected graphlets  $G_1$  and  $G_2$ , six 4-node undirected graphlets  $G_3, \dots, G_8$ , and thirteen 3-node directed graphlets  $G_1^{(3d)}, \dots, G_{13}^{(3d)}$ . Nodes may occupy very different positions in the same graphlet. For example, the three leaf nodes (in black) of  $G_4$  are symmetric, and the other node (in white) of  $G_4$  exhibits more like a hub. According to the positions that nodes of a graphlet occupies, the graphlet's nodes are classified into one or more different orbits (i.e., position classes) associated with them. The values of orbit IDs have no specific meaning, and we set the values of orbit IDs same as [1].

3D are several orders of magnitude faster than state-of-the-art enumeration methods for accurately estimating graphlet orbit degrees. We demonstrate the ability of SAND and SAND-3D to explore large graphs with millions of nodes and edges. To guarantee reproducibility of the experimental results, we release the source code of SAND in open source<sup>2</sup>.

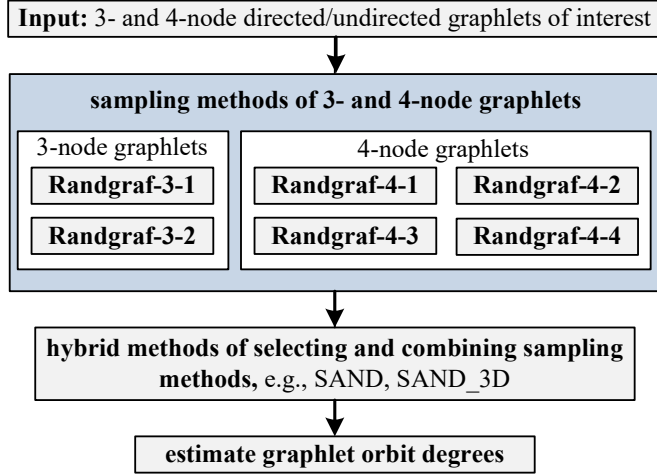


**Figure 2: Overview of our methods.**

The rest of this paper is organized as follows. Section 2 presents the problem formulation. Section 3 introduces preliminaries used in this paper. Section 4 presents our methods (i.e., Randgraf-3-1, Randgraf-3-2, Randgraf-4-1, Randgraf-4-2, Randgraf-4-3, and Randgraf-4-4) for sampling 3- and 4-node CISes including a given

<sup>2</sup><http://nskeylab.xjtu.edu.cn/dataset/phwang/code>

node. Sections 5 and 6 present our methods SAND and SAND-3D for estimating undirected and directed graphlet orbit degrees respectively. Section 7 presents the performance evaluation and testing results. Section 8 summarizes related work. Concluding remarks then follow.

## 2. PROBLEM FORMULATION

Denote the underlying graph of interest as  $G = (V, E, L)$ , where  $V$  is a set of nodes,  $E$  is a set of **undirected** edges,  $E \in V \times V$ , and  $L$  is a set of edge directions  $\{l_{u,v} : (u,v) \in E\}$ , where we attach a label  $l_{u,v} \in \{\rightarrow, \leftarrow, \leftrightarrow\}$  to indicate the direction of  $(u,v) \in E$  for a directed network. If  $L$  is empty, then  $G$  is an undirected graph.

In order to define graphlet orbit degrees, we first introduce some notation. A subgraph  $G'$  of  $G$  is a graph whose set of nodes, set of edges, and set of edge directions are all subsets of  $G$ . An induced subgraph of  $G$ ,  $G' = (V', E', L')$ , is a subgraph that consists of a subset of nodes in  $G$  and **all of the edges** that connect them in  $G$ , i.e.  $V' \subset V$ ,  $E' = \{(u,v) : u,v \in V', (u,v) \in E\}$ ,  $L' = \{l_{u,v} : u,v \in V', (u,v) \in E\}$ . **Unless we explicitly say "induced" in this paper, a subgraph is not necessarily induced.** Fig. 1(a) shows all 2-, 3-, and 4-node undirected graphlets  $G_i$ ,  $0 \leq i \leq 8$ , in [1]. By taking into account the "symmetries" between nodes in  $G_i$ , [1] classifies the nodes of  $G_i$  into different automorphism **orbits** (or just orbits, for brevity), where the nodes with the same orbit ID are topologically identical. For all  $G_i$ ,  $0 \leq i \leq 8$ , there are 15 orbits, which are shown in Fig. 1(a). Denote  $C_v^{(i)}$  as the set of connected and induced subgraphs (CISes) in  $G$  that touch a node  $v \in V$  at orbit  $i$ . Let  $d_v^{(i)} = |C_v^{(i)}|$  denote the **graphlet orbit  $i$  degree** (or just "**orbit  $i$  degree**", for brevity) of  $v$ . The graphlet orbit degree vector,  $(d_v^{(0)}, \dots, d_v^{(14)})$ , can be used as a signature of node  $v$  for applications such as identifying similar nodes. We observe that  $C_v^{(0)}$  contains the edges in  $G$  that includes node  $v$ , i.e.,  $C_v^{(0)} = \{(u,v) : (u,v) \in E\}$ , and  $d_v^{(0)}$  is the number of neighbors

of  $v$ . For simplicity, we denote  $d_v = d_v^{(0)}$  as the degree of node  $v$ . An example is given in Fig. 3, where  $d_v^{(0)} = 3$ ,  $d_v^{(2)} = 2$ ,  $d_v^{(1)} = d_v^{(3)} = d_v^{(5)} = d_v^{(10)} = d_v^{(11)} = 1$ , and  $d_v^{(4)} = d_v^{(6)} = d_v^{(7)} = d_v^{(8)} = d_v^{(9)} = d_v^{(12)} = d_v^{(13)} = d_v^{(14)} = 0$ . The concept of orbit and graphlet orbit degree extends to directed graphs, as shown in Fig. 1(b), directed graphs have thirteen 3-node graphlets  $G_1^{(3d)}$  whose nodes are distributed at 30 different orbits. In this paper we focus on 3-node directed graphlets and orbits because of the large number of directed 4-node graphlets and orbits.

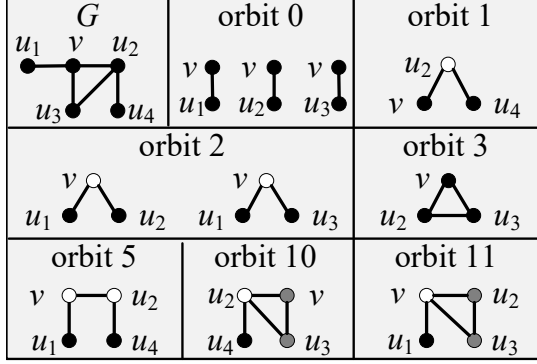


**Figure 3: Example of computing the undirected orbit degrees of node  $v$  in the undirected graph  $G$ .**

As discussed above, it is computationally intensive to enumerate and count all 3- and 4-node CISEs that include a given node with a large number of neighbors in large graphs. For example, later our experiments show that the node with the largest degree in graph Wiki-Talk [12] belongs to more than  $10^{14}$  3- and 4-node CISEs. In this paper, we develop efficient methods to estimate graphlet orbit degrees and identify orbits with the largest graphlet orbit degrees for undirected and directed graphs. For ease of reading, we list notation used throughout the paper in Table 1 and we present the proofs of all our theorems in Appendix.

### 3. PRELIMINARIES

In this section, we introduce two theorems that provide the foundation for our methods of estimating graphlet orbit degrees.

**THEOREM 1. (Estimating subset cardinalities)** Let  $S_1, \dots, S_r$  be a non-overlapping division of a set  $S$  of interest, i.e.,  $S = S_1 \cup \dots \cup S_r$  and  $S_i \cap S_j = \emptyset, i \neq j, i, j = 1, \dots, r$ . Let  $n_i = |S_i|$  denote the cardinality of  $S_i, 1 \leq i \leq r$ . Suppose there exists a function  $\mathbb{F}$  that returns an item  $X$  sampled from  $S$  according to a distribution  $P(X = s, s \in S_i) = p_i$ , where  $\sum_{i=1}^r n_i p_i = 1$ . Let  $X_1, \dots, X_K$  be items obtained by calling function  $\mathbb{F}$   $K$  times independently. Denote by  $\mathbf{1}(\mathbb{X})$  the indicator function that equals one when predicate  $\mathbb{X}$  is true, and zero otherwise. When  $p_i > 0$ , we can estimate  $n_i$  as:

$$\hat{n}_i = \frac{\sum_{j=1}^K \mathbf{1}(X_j \in S_i)}{K p_i}, \quad 1 \leq i \leq r,$$

where  $\hat{n}_i$  is an **unbiased** estimator of  $n_i$ , i.e.,  $\mathbb{E}(\hat{n}_i) = n_i$  with variance  $\text{Var}(\hat{n}_i) = \frac{n_i}{K} \left( \frac{1}{p_i} - n_i \right)$ . The covariance of  $\hat{n}_i$  and  $\hat{n}_j$  is  $\text{Cov}(\hat{n}_i, \hat{n}_j) = -\frac{n_i n_j}{K}, i \neq j, i, j = 1, \dots, r$ .

**THEOREM 2. (Combining unbiased estimators[13])** Suppose there exist  $k$  **independent** and **unbiased** estimates  $c_1, \dots, c_k$  of  $c$  with variances  $\text{Var}(c_j), j = 1, \dots, k$ . The estimate  $\hat{c} = \sum_{j=1}^k \alpha_j c_j$

**Table 1: Table of notation.**

$G = (V, E, L)$	$G$ is the graph of interest
$N_v$	the set of neighbors of a node $v$ in $G$
$d_v$	$d_v =  N_v $ , the cardinality of set $N_v$
$G_0, \dots, G_8$	2-, 3-, and 4-node undirected graphlets
$G_1^{3d}, \dots, G_{13}^{3d}$	3-node directed graphlets
$d_v^{(1)}, \dots, d_v^{(14)}$	undirected orbit degrees of node $v$
$d_v^{(1,dir)}, \dots, d_v^{(30,dir)}$	directed orbit degrees of node $v$
$p_1^{(3,1)}, \dots, p_{14}^{(3,1)}$	probability distribution of methods
$p_1^{(3,2)}, \dots, p_{14}^{(3,2)}$	Randgraf-3-1, Randgraf-3-2,
$p_1^{(4,1)}, \dots, p_{14}^{(4,1)}$	Randgraf-4-1, Randgraf-4-2,
$p_1^{(4,2)}, \dots, p_{14}^{(4,2)}$	Randgraf-4-3, and Randgraf-4-4
$p_1^{(4,3)}, \dots, p_{14}^{(4,3)}$	sampling undirected orbits 1–14
$p_1^{(4,4)}, \dots, p_{14}^{(4,4)}$	respectively
$K^{(3,1)}, K^{(3,2)}, K^{(4,1)}, K^{(4,2)}, K^{(4,3)}, K^{(4,4)}$	sampling budgets of Randgraf-3-1, Randgraf-3-2, Randgraf-4-1, Randgraf-4-2, Randgraf-4-3, and Randgraf-4-4
$\alpha^{(v)} = \{\alpha_u^{(v)} = \frac{d_u - 1}{\varphi_u} : u \in N_v\}$	
$\beta^{(v)} = \{\beta_u^{(v)} = \frac{\varphi_u - d_u + 1}{\Phi_v^{(2)}} : u \in N_v\}$	
$\gamma^{(v)} = \{\gamma_u^{(v)} = \frac{\varphi_u - d_u + 1}{\Phi_v^{(3)}} : u \in N_v\}$	
$\rho^{(u,v)} = \{\rho_w^{(u,v)} = \frac{d_w - 1}{\varphi_w - d_u + 1} : w \in N_u - \{v\}\}$	
$\phi_v = \frac{d_v(d_v - 1)}{2}, \varphi_v = \sum_{u \in N_v} (d_u - 1)$	
$\Phi_v^{(1)} = (d_v - 1)\varphi_v, \Phi_v^{(2)} = \sum_{u \in N_v} (\phi_u - d_u + 1)$	
$\Phi_v^{(3)} = \sum_{u \in N_v} (\varphi_u - d_v + 1), \Phi_v^{(4)} = \frac{d_v(d_v - 1)(d_v - 2)}{6}$	

where  $\alpha_i = \frac{\text{Var}^{-1}(c_i)}{\sum_{j=1}^k \text{Var}^{-1}(c_j)}$  is the minimum variance estimate based on a linear combination of  $c_1, \dots, c_k$ . It has variance  $\text{Var}(\hat{c}) = \frac{1}{\sum_{j=1}^k \text{Var}^{-1}(c_j)}$ .

### 4. SAMPLING 3- AND 4-NODE CISES

In this section, we first present the basic idea and then present methods for sampling 3- and 4-node CISEs. **Basic idea behind our methods:** Let  $S(v)$  denote the set of all 3- and 4-node CISEs that include a given node  $v \in V$  of interest. Let  $S_i(v) \in S(v)$  denote the set of CISEs that include  $v$  in undirected orbit  $i = 1, \dots, 14$  (Fig. 1(a)). According to Theorem 1, the key to estimating orbit degrees of  $v$  is to design a fast method to sample CISEs from  $S(v)$  whose sampling probability distribution  $P(X = s, s \in S_i), 1 \leq i \leq r$ , can be easily derived and computed. Our sampling methods are performed on the undirected graphs of  $G$ . The "orbit" mentioned in this section refers to the "undirected orbit". These sampling methods are used as building blocks for graphlet statistics estimation methods presented in Sections 5 and 6.

#### 4.1 Methods for Sampling 3-Node CISEs

We develop two efficient sampling methods  $\text{Randgraf-3-1}(v, G)$  and  $\text{Randgraf-3-2}(v, G)$  to sample 3-node CISEs in  $G$  that include  $v$ .  $\text{Randgraf-3-1}(v, G)$  is able to sample 3-node CISEs that include  $v$  in orbits 2 and 3.  $\text{Randgraf-3-2}(v, G)$  is able to sample 3-node CISEs that include  $v$  in orbits 1 and 3. Next, we introduce  $\text{Randgraf-3-1}(v, G)$  and  $\text{Randgraf-3-2}(v, G)$  respectively.

**Method Randgraf-3-1**( $v, G$ ): To sample a CIS that includes  $v$ ,  $\text{Randgraf-3-1}(v, G)$  consists of three steps: **Step 1**) Sample node  $u$  from  $N_v$  (i.e., the neighbors of  $v$ ) at random; **Step 2**) Sample

node  $w$  from  $N_v \setminus \{u\}$  at random; **Step 3**) Return CIS  $s$  consisting of nodes  $v, u,$  and  $w$ . The pseudo-code for Randgraf-3-1( $v, G$ ) is shown in Algorithm 1. Theorem 3 specifies the sampling bias of Randgraf-3-1( $v, G$ ), which is critical for estimating graphlet orbit degrees of  $v$ .

---

**Algorithm 1:** The pseudo-code of Randgraf-3-1( $v, G$ ).

---

**input** :  $G = (V, E, L)$  and  $v \in V$ .  
**output**: a 3-node CIS  $s$  that includes  $v$ .  
 $u \leftarrow \text{RandomVertex}(N_v)$ ;  
 $w \leftarrow \text{RandomVertex}(N_v \setminus \{u\})$ ;  
 $s \leftarrow \text{CIS}(\{v, u, w\})$ ;

---

**THEOREM 3.** Let  $p_i^{(3,1)}$ ,  $i \in \{1, 2, 3\}$ , denote the probability that method Randgraf-3-1 samples a 3-node CIS  $s$  including  $v$  in orbit  $i$ . Then  $p_1^{(3,1)} = 0$ ,  $p_2^{(3,1)} = \frac{1}{\phi_v}$ , and  $p_3^{(3,1)} = \frac{1}{\phi_v}$ , where  $\phi_v = \frac{d_v(d_v-1)}{2}$ .

**Method Randgraf-3-2( $v, G$ ):** Define  $\varphi_v = \sum_{u \in N_v} (d_u - 1)$  and  $\alpha_u^{(v)} = \frac{d_u-1}{\varphi_v}$ . To sample a 3-node CIS that includes  $v$ , method Randgraf-3-2( $v, G$ ) consists of three steps: **Step 1**) Sample node  $u$  from  $N_v$  according to distribution  $\alpha^{(v)} = \{\alpha_u^{(v)} : u \in N_v\}$ . Here we do not sample  $u$  from  $N_v$  uniformly but according to  $\alpha^{(v)}$  to facilitate estimation of the sampling bias; **Step 2**) Sample node  $w$  from  $N_u \setminus \{v\}$  at random; **Step 3**) Return CIS  $s$  consisting of nodes  $v, u,$  and  $w$ . Algorithm 2 shows the pseudo-code for Randgraf-3-2( $v, G$ ). Function  $\text{WeightRandomVertex}(N_v, \alpha^{(v)})$  in Algorithm 2 returns a node sampled from  $N_v$  according to distribution  $\alpha^{(v)} = \{\alpha_u^{(v)} : u \in N_v\}$ . Theorem 4 specifies the sampling bias of Randgraf-3-2( $v, G$ ).

---

**Algorithm 2:** The pseudo-code of Randgraf-3-2( $v, G$ ).

---

**input** :  $G = (V, E, L)$  and  $v \in V$ .  
**output**: a 3-node CIS  $s$  that includes  $v$ .  
 $u \leftarrow \text{WeightRandomVertex}(N_v, \alpha^{(v)})$ ;  
 $w \leftarrow \text{RandomVertex}(N_u \setminus \{v\})$ ;  
 $s \leftarrow \text{CIS}(\{v, u, w\})$ ;

---

**THEOREM 4.** Let  $p_i^{(3,2)}$ ,  $i \in \{1, 2, 3\}$ , denote the probability that method Randgraf-3-2 samples a 3-node CIS  $s$  including  $v$  in orbit  $i$ . Then  $p_1^{(3,2)} = \frac{1}{\varphi_v}$ ,  $p_2^{(3,2)} = 0$ , and  $p_3^{(3,2)} = \frac{2}{\varphi_v}$ .

## 4.2 Methods for Sampling 4-Node CISes

In this subsection, we develop four methods: Randgraf-4-1( $v, G$ ), Randgraf-4-2( $v, G$ ), Randgraf-4-3( $v, G$ ), and Randgraf-4-4( $v, G$ ) to sample 4-node CISes in  $G$  that include  $v$ . Each of these four methods is only able to sample 4-node CISes that include  $v$  in a subset of orbits. However, together they are able to sample all 4-node CISes that include  $v$ . We introduce these four methods below.

**Method Randgraf-4-1( $v, G$ ):** To sample a 4-node CIS that includes  $v$ , method Randgraf-4-1( $v, G$ ) consists of four steps: **Step 1**) Sample node  $u$  from  $N_v$  according to distribution  $\alpha^{(v)} = \{\alpha_u^{(v)} : u \in N_v\}$ ; **Step 2**) Sample node  $w$  from  $N_v \setminus \{u\}$  at random; **Step 3**) Sample node  $r$  from  $N_u \setminus \{v\}$  at random; **Step 4**) Return CIS  $s$  consisting of nodes  $v, u, w,$  and  $r$ . Note that  $s$  is a 3-node CIS when  $w = r$ . The pseudo-code for Randgraf-4-1( $v, G$ ) is shown in Algorithm 3. Theorem 5 states the sampling bias of Randgraf-4-1( $v, G$ ), where  $\Phi_v^{(1)} = (d_v - 1)\varphi_v$ .

---

**Algorithm 3:** The pseudo-code of Randgraf-4-1( $v, G$ ).

---

**input** :  $G = (V, E, L)$  and  $v \in V$ .  
**output**: a 3- or 4-node CIS  $s$  that includes  $v$ .  
 $u \leftarrow \text{WeightRandomVertex}(N_v, \alpha^{(v)})$ ;  
 $w \leftarrow \text{RandomVertex}(N_v \setminus \{u\})$ ;  
 $r \leftarrow \text{RandomVertex}(N_u \setminus \{v\})$ ;  
 $s \leftarrow \text{CIS}(\{v, u, w, r\})$ ;

---

**THEOREM 5.** Let  $p_i^{(4,1)}$ ,  $i \in \{1, \dots, 14\}$ , denote the probability that method Randgraf-4-1 samples a 3- or 4-node CIS  $s$  including  $v$  in orbit  $i$ . Then  $p_1^{(4,1)} = p_2^{(4,1)} = p_4^{(4,1)} = p_6^{(4,1)} = p_7^{(4,1)} = p_9^{(4,1)} = 0$ ,  $p_3^{(4,1)} = \frac{2}{\Phi_v^{(1)}}$ ,  $p_5^{(4,1)} = \frac{1}{\Phi_v^{(1)}}$ ,  $p_8^{(4,1)} = \frac{2}{\Phi_v^{(1)}}$ ,  $p_{10}^{(4,1)} = \frac{1}{\Phi_v^{(1)}}$ ,  $p_{11}^{(4,1)} = \frac{2}{\Phi_v^{(1)}}$ ,  $p_{12}^{(4,1)} = \frac{2}{\Phi_v^{(1)}}$ ,  $p_{13}^{(4,1)} = \frac{4}{\Phi_v^{(1)}}$ , and  $p_{14}^{(4,1)} = \frac{6}{\Phi_v^{(1)}}$ .

**Method Randgraf-4-2( $v, G$ ):** Define  $\Phi_v^{(2)} = \sum_{u \in N_v} (\phi_u - d_u + 1)$  and  $\beta_u^{(v)} = \frac{\phi_u - d_u + 1}{\Phi_v^{(2)}}$ . To sample a 4-node CIS that includes  $v$ , Randgraf-4-2( $v, G$ ) consists of four steps: **Step 1**) Sample node  $u$  from  $N_v$  according to distribution  $\beta^{(v)} = \{\beta_u^{(v)} : u \in N_v\}$ ; **Step 2**) Sample node  $w$  from  $N_u \setminus \{v\}$  at random; **Step 3**) Sample node  $r$  from  $N_u \setminus \{v, u\}$  at random; **Step 4**) Return CIS  $s$  consisting of nodes  $v, u, w,$  and  $r$ . Theorem 6 states the sampling bias of Randgraf-4-2( $v, G$ ).

---

**Algorithm 4:** The pseudo-code of Randgraf-4-2( $v, G$ ).

---

**input** :  $G = (V, E, L)$  and  $v \in V$ .  
**output**: a 4-node CIS  $s$  that includes  $v$ .  
 $u \leftarrow \text{WeightRandomVertex}(N_v, \beta^{(v)})$ ;  
 $w \leftarrow \text{RandomVertex}(N_u \setminus \{v\})$ ;  
 $r \leftarrow \text{RandomVertex}(N_u \setminus \{v, u\})$ ;  
 $s \leftarrow \text{CIS}(\{v, u, w, r\})$ ;

---

**THEOREM 6.** Let  $p_i^{(4,2)}$ ,  $i \in \{1, \dots, 14\}$ , denote the probability that method Randgraf-4-2 samples a 4-node CIS  $s$  including  $v$  in orbit  $i$ . Then  $p_1^{(4,2)} = p_2^{(4,2)} = p_3^{(4,2)} = p_4^{(4,2)} = p_5^{(4,2)} = p_7^{(4,2)} = p_8^{(4,2)} = p_{11}^{(4,2)} = 0$ ,  $p_6^{(4,2)} = \frac{1}{\Phi_v^{(2)}}$ ,  $p_9^{(4,2)} = \frac{1}{\Phi_v^{(2)}}$ ,  $p_{10}^{(4,2)} = \frac{1}{\Phi_v^{(2)}}$ ,  $p_{12}^{(4,2)} = \frac{2}{\Phi_v^{(2)}}$ ,  $p_{13}^{(4,2)} = \frac{1}{\Phi_v^{(2)}}$ , and  $p_{14}^{(4,2)} = \frac{3}{\Phi_v^{(2)}}$ .

**Method Randgraf-4-3( $v, G$ ):** Define  $\Phi_v^{(3)} = \sum_{u \in N_v} (\varphi_u - d_v + 1)$ ,  $\gamma_u^{(v)} = \frac{\varphi_u - d_v + 1}{\Phi_v^{(3)}}$ , and  $\rho_w^{(u,v)} = \frac{d_w - 1}{\varphi_u - d_v + 1}$ . To sample a 4-node CIS that includes  $v$ , method Randgraf-4-3( $v, G$ ) consists of four steps: **Step 1**) Sample node  $u$  from  $N_v$  according to distribution  $\gamma^{(v)} = \{\gamma_u^{(v)} : u \in N_v\}$ ; **Step 2**) Sample node  $w$  from  $N_u \setminus \{v\}$  according to distribution  $\rho^{(u,v)} = \{\rho_w^{(u,v)} : w \in N_u \setminus \{v\}\}$ ; **Step 3**) Sample node  $r$  from  $N_w \setminus \{u\}$  at random; **Step 4**) Return CIS  $s$  consisting of nodes  $v, u, w,$  and  $r$ . Note that  $s$  is a 3-node CIS when  $r = v$ . The pseudo-code for Randgraf-4-3( $v, G$ ) is shown in Algorithm 5. Theorem 7 states the sampling bias of Randgraf-4-3( $v, G$ ).

**THEOREM 7.** Let  $p_i^{(4,3)}$ ,  $i \in \{1, \dots, 14\}$ , denote the probability that method Randgraf-4-3 samples a 3- or 4-node CIS  $s$  including  $v$  in orbit  $i$ . Then  $p_1^{(4,3)} = p_2^{(4,3)} = p_5^{(4,3)} = p_6^{(4,3)} =$

---

**Algorithm 5:** The pseudo-code of Randgraf-4-3( $v, G$ ).

---

**input** :  $G = (V, E, L)$  and  $v \in V$ .  
**output**: a 3- or 4-node CIS  $s$  that includes  $v$ .  
 $u \leftarrow \text{WeightRandomVertex}(N_v, \gamma^{(v)});$   
 $w \leftarrow \text{WeightRandomVertex}(N_u \setminus \{v\}, \rho^{(u,v)});$   
 $r \leftarrow \text{RandomVertex}(N_w \setminus \{u\});$   
 $s \leftarrow \text{CIS}(\{v, u, w, r\});$

---

$$p_7^{(4,3)} = p_{11}^{(4,3)} = 0, p_3^{(4,3)} = \frac{2}{\Phi_v^{(3)}}, p_4^{(4,3)} = \frac{1}{\Phi_v^{(3)}}, p_8^{(4,3)} = \frac{2}{\Phi_v^{(3)}},$$

$$p_9^{(4,3)} = \frac{2}{\Phi_v^{(3)}}, p_{10}^{(4,3)} = \frac{1}{\Phi_v^{(3)}}, p_{12}^{(4,3)} = \frac{4}{\Phi_v^{(3)}}, p_{13}^{(4,3)} = \frac{2}{\Phi_v^{(3)}}, \text{ and}$$

$$p_{14}^{(4,3)} = \frac{6}{\Phi_v^{(3)}}.$$

**Method Randgraf-4-4**( $v, G$ ): To sample a 4-node CIS that includes  $v$ , method Randgraf-4-4( $v, G$ ) consists of four steps: **Step 1**) Sample node  $u$  from  $N_v$  at random; **Step 2**) Sample node  $w$  from  $N_v \setminus \{u\}$  at random; **Step 3**) Sample node  $r$  from  $N_v \setminus \{v, u\}$  at random; **Step 4**) Return CIS  $s$  consisting of nodes  $v, u, w$ , and  $r$ . The pseudo-code for Randgraf-4-4( $v, G$ ) is shown in Algorithm 6. Theorem 8 states the sampling bias of Randgraf-4-4( $v, G$ ), where  $\Phi_v^{(4)} = \frac{d_v(d_v-1)(d_v-2)}{6}$ .

---

**Algorithm 6:** The pseudo-code of Randgraf-4-4( $v, G$ ).

---

**input** :  $G = (V, E, L)$  and  $v \in V$  with  $d_v \geq 3$ .  
**output**: a 4-node CIS  $s$  that includes  $v$ .  
 $u \leftarrow \text{RandomVertex}(N_v);$   
 $w \leftarrow \text{RandomVertex}(N_v \setminus \{u\});$   
 $r \leftarrow \text{RandomVertex}(N_v \setminus \{u, v\});$   
 $s \leftarrow \text{CIS}(\{v, u, w, r\});$

---

**THEOREM 8.** Let  $p_i^{(4,4)}$ ,  $i \in \{1, \dots, 14\}$ , denote the probability that method Randgraf-4-4 samples a 3- or 4-node CIS  $s$  including  $v$  in orbit  $i$ . Then  $p_1^{(4,4)} = p_2^{(4,4)} = p_3^{(4,4)} = p_4^{(4,4)} = p_5^{(4,4)} = p_6^{(4,4)} = p_8^{(4,4)} = p_9^{(4,4)} = p_{10}^{(4,4)} = p_{12}^{(4,4)} = 0$ , and  $p_7^{(4,4)} = p_{11}^{(4,4)} = p_{13}^{(4,4)} = p_{14}^{(4,4)} = \frac{1}{\Phi_v^{(4)}}$ .

### 4.3 Discussion

The details of implementing the functions in the Algorithms we presented subsections 4.1 and 4.2 and analyzing their computational complexities are discussed in Appendix. Table 2 summarizes and compares Randgraf-3-1, Randgraf-3-2, Randgraf-4-1, Randgraf-4-2, Randgraf-4-3, and Randgraf-4-4. We observe that 1) each method is not able to sample "all" CISes that includes  $v$ . CISes that includes  $v$  in orbits 2, 1, 5, 6, 4, and 7 can only be sampled by Randgraf-3-1, Randgraf-3-2, Randgraf-4-1, Randgraf-4-2, Randgraf-4-3, and Randgraf-4-4 respectively. Thus, all six methods are needed to guarantee each CIS that includes  $v$  is sampled with probability larger than zero; 2) Randgraf-4-1, Randgraf-4-2, and Randgraf-4-3 are able to sample CISes that includes  $v$  in more orbits than Randgraf-4-4; 3) Randgraf-4-3 exhibits the highest computational complexity than the other methods.

## 5. SAND: ESTIMATION OF UNDIRECTED ORBIT DEGREES

In this section, we present orbit degree estimators based on the above sampling methods. We first focus on a single undirected orbit and then modify it to estimate the degrees of all undirected orbits.

### 5.1 Estimating Single Undirected Orbit Degree

Consider the problem of estimating the orbit  $i$  degree. If undirected orbit  $i$  can only be sampled by one method in Section 3 (e.g., Randgraf-3-2 is the only that samples orbit 1), we use that method to obtain  $K$  CISes that include node  $v \in V$ . Let  $p_i$  be the probability that the method samples a CIS in orbit  $i$ , and let  $m_i$  denote the number of sampled CISes that include  $v$  in orbit  $i$ . According to Theorem 1, we estimate  $d_v^{(i)}$  as

$$\hat{d}_v^{(i)} = \frac{m_i}{K p_i},$$

and the variance of  $\hat{d}_v^{(i)}$  is  $\text{Var}(\hat{d}_v^{(i)}) = \frac{d_v^{(i)}}{K} \left( \frac{1}{p_i} - d_v^{(i)} \right)$ . When more than one method is able to sample undirected orbit  $i$ , we select the most efficient method, the one with the smallest  $\frac{\text{Var}(\hat{d}_v^{(i)})}{K t_v}$  to estimate  $d_v^{(i)}$ , where  $t_v$  is the average computational time of the method sampling a CIS.

### 5.2 Estimating all Undirected Orbit Degrees

We observe that **the relationships between undirected orbit degrees can be used to reduce the sampling cost of estimating all undirected orbit degrees**. For example, the following Theorem 9 show that  $d_v^{(2)} + d_v^{(3)} = \phi_v$ . When one has obtained an accurate estimate of  $d_v^{(3)}$ , it is not necessary to apply the sampling method in Section 5.1 to estimate  $d_v^{(2)}$  since  $d_v^{(2)}$  can be computed according to the above equation.

**THEOREM 9.** We have the following relations for a node  $v \in V$  in undirected graph  $G$

$$d_v^{(2)} + d_v^{(3)} = \phi_v, \quad (1)$$

$$2d_v^{(3)} + d_v^{(4)} + 2d_v^{(8)} + 2d_v^{(9)} + d_v^{(10)} + 4d_v^{(12)} + 2d_v^{(13)} + 6d_v^{(14)} = \Phi_v^{(3)}, \quad (2)$$

$$d_v^{(7)} + d_v^{(11)} + d_v^{(13)} + d_v^{(14)} = \Phi_v^{(4)}. \quad (3)$$

We develop a fast method SAND consisting of Randgraf-3-2, Randgraf-4-1, Randgraf-4-2 to estimate all 3- and 4-node undirected orbit degrees inspired by the following observations:

**Observation 1.** For node  $v$  with the largest degree in  $G$ , we observe  $d_v^{(2)} \gg d_v^{(1)}$  and  $d_v^{(2)} \gg d_v^{(3)}$  for most real-world networks. Then, we find that Randgraf-3-2 is more efficient for estimating  $d_v^{(3)}$  than Randgraf-3-1 because Randgraf-3-1 rarely samples undirected orbit 3. Similarly, we observe that Randgraf-4-1, Randgraf-4-2, Randgraf-4-3, and Randgraf-4-4 never or rarely sample undirected orbit 3.

**Observation 2.** Randgraf-4-1( $v, G$ ) and Randgraf-4-2( $v, G$ ) together can sample 4-node CISes that include  $v$  in undirected orbits  $i \in \{4, \dots, 14\} \setminus \{4, 7\}$ .

**Observation 3.** Theorem 9 presents three relationships between undirected orbit degrees, which enable us to estimate undirect orbit  $i \in \{2, 4, 7\}$  degrees.

Formally, SAND consists of the following three steps:

**Step 1:** Apply function Randgraf-3-2( $v, G$ )  $K^{(3,2)}$  times to sample  $K^{(3,2)}$  CISes, and then count the number of sampled CISes that include  $v$  in undirected orbit  $i \in \{1, 2, 3\}$ , denoted as  $m_i^{(3,2)}$ ;

**Step 2:** Apply Randgraf-4-1( $v, G$ )  $K^{(4,1)}$  times to sample  $K^{(4,1)}$  CISes, and then count the number of sampled CISes that include  $v$  in undirected orbit  $i \in \{1, \dots, 14\}$ , denoted as  $m_i^{(4,1)}$ ;

**Step 3:** Apply function Randgraf-4-2( $v, G$ )  $K^{(4,2)}$  times to sample

**Table 2: Summary of graphlet orbit sampling methods in this paper.**

method	whether the method is able to sample a CIS that includes $v$ in orbit $i$														computational complexity	
	1	2	3	4	5	6	7	8	9	10	11	12	13	14	initialization	sample one CIS
Randgraf-3-1( $v, G$ )	×	✓	✓	×	×	×	×	×	×	×	×	×	×	×	0	$O(1)$
Randgraf-3-2( $v, G$ )	✓	×	✓	×	×	×	×	×	×	×	×	×	×	×	0	$O(\log d_v)$
Randgraf-4-1( $v, G$ )	×	×	✓	×	✓	×	×	✓	×	✓	✓	✓	✓	✓	$O(d_v)$	$O(\log d_v)$
Randgraf-4-2( $v, G$ )	×	×	×	×	×	✓	×	×	✓	✓	×	✓	✓	✓	$O(d_v)$	$O(\log d_v)$
Randgraf-4-3( $v, G$ )	×	×	✓	✓	×	×	×	✓	✓	✓	×	✓	✓	✓	$O(d_v + \sum_{u \in N_v} d_u)$	$O(\log d_v + \sum_{u \in N_v} \pi_u^{(v)} \log d_u)$
Randgraf-4-4( $v, G$ )	×	×	×	×	×	×	✓	×	×	×	✓	×	✓	✓	0	$O(1)$

$K^{(4,2)}$  CISes, and then count the number of sampled CISes that include  $v$  in undirected orbit  $i \in \{1, \dots, 14\}$ , denoted as  $m_i^{(4,2)}$ .

Next, we estimate  $d_v^{(1)}, \dots, d_v^{(14)}$  as follows:

**Step 1:** For undirected orbit  $i \in \{1, 5, 6, 8, 9, 11\}$ , we estimate  $d_v^{(i)}$  as

$$\hat{d}_v^{(i)} = \begin{cases} \frac{m_1^{(3,2)}}{K^{(3,2)} p_2^{(3,2)}}, & i = 1, \\ \frac{m_i^{(4,1)}}{K^{(4,1)} p_i^{(4,1)}}, & i \in \{5, 8, 11\}, \\ \frac{m_i^{(4,2)}}{K^{(4,2)} p_i^{(4,2)}}, & i \in \{6, 9\}; \end{cases} \quad (4)$$

**Step 2:** For undirected orbit 3, we compute two estimates  $\hat{d}_v^{(3)} = \frac{m_3^{(4,1)}}{K^{(4,1)} p_3^{(4,1)}}$  and  $\tilde{d}_v^{(3)} = \frac{m_3^{(3,2)}}{K^{(3,2)} p_3^{(3,2)}}$ . According to Theorem 1, these are unbiased estimates of  $d_v^{(3)}$  and their variances are

$$\text{Var}(\tilde{d}_v^{(3)}) = \frac{d_v^{(3)}}{K^{(4,1)}} \left( \frac{1}{p_3^{(4,1)}} - d_v^{(3)} \right), \quad (5)$$

$$\text{Var}(\hat{d}_v^{(3)}) = \frac{d_v^{(3)}}{K^{(3,2)}} \left( \frac{1}{p_3^{(3,2)}} - d_v^{(3)} \right). \quad (6)$$

Theorem 2 allows us to compute the more accurate estimate

$$\hat{d}_v^{(3)} = \lambda_v^{(3,1)} \tilde{d}_v^{(3)} + \lambda_v^{(3,2)} \hat{d}_v^{(3)}, \quad (7)$$

where  $\lambda_v^{(3,1)} = \frac{\text{Var}(\hat{d}_v^{(3)})}{\text{Var}(\tilde{d}_v^{(3)}) + \text{Var}(\hat{d}_v^{(3)})}$  and  $\lambda_v^{(3,2)} = \frac{\text{Var}(\tilde{d}_v^{(3)})}{\text{Var}(\tilde{d}_v^{(3)}) + \text{Var}(\hat{d}_v^{(3)})}$  with  $\text{Var}(\tilde{d}_v^{(3)})$  and  $\text{Var}(\hat{d}_v^{(3)})$  given by replacing  $d_v^{(3)}$  with  $\tilde{d}_v^{(3)}$  and  $\hat{d}_v^{(3)}$  in Eqs. (5) and (6);

**Step 3:** For undirected orbit  $i \in \{10, 12, 13, 14\}$ , we use Theorem 1 to compute two estimates  $\tilde{d}_v^{(i)} = \frac{m_i^{(4,1)}}{K^{(4,1)} p_i^{(4,1)}}$  and  $\hat{d}_v^{(i)} = \frac{m_i^{(4,2)}}{K^{(4,2)} p_i^{(4,2)}}$  with variances

$$\text{Var}(\tilde{d}_v^{(i)}) = \frac{d_v^{(i)}}{K^{(4,1)}} \left( \frac{1}{p_i^{(4,1)}} - d_v^{(i)} \right), \quad (8)$$

$$\text{Var}(\hat{d}_v^{(i)}) = \frac{d_v^{(i)}}{K^{(4,2)}} \left( \frac{1}{p_i^{(4,2)}} - d_v^{(i)} \right). \quad (9)$$

We then apply Theorem 2 to compute the more accurate estimate

$$\hat{d}_v^{(i)} = \lambda_v^{(i,1)} \tilde{d}_v^{(i)} + \lambda_v^{(i,2)} \hat{d}_v^{(i)}, \quad (10)$$

where  $\lambda_v^{(i,1)} = \frac{\text{Var}(\hat{d}_v^{(i)})}{\text{Var}(\tilde{d}_v^{(i)}) + \text{Var}(\hat{d}_v^{(i)})}$  and  $\lambda_v^{(i,2)} = \frac{\text{Var}(\tilde{d}_v^{(i)})}{\text{Var}(\tilde{d}_v^{(i)}) + \text{Var}(\hat{d}_v^{(i)})}$  obtained by replacing  $d_v^{(i)}$  with  $\tilde{d}_v^{(i)}$  and  $\hat{d}_v^{(i)}$  in Eqs. (8) and (9);

**Step 4:** For undirected orbit  $i \in \{2, 4, 7\}$ , we now estimate  $d_v^{(i)}$  as

$$\hat{d}_v^{(2)} = \phi_v - \hat{d}_v^{(3)},$$

$$\hat{d}_v^{(4)} = \Phi_v^{(3)} - 2\hat{d}_v^{(3)} - 2\hat{d}_v^{(8)} - 2\hat{d}_v^{(9)} - \hat{d}_v^{(10)} - 4\hat{d}_v^{(12)} - 2\hat{d}_v^{(13)} - 6\hat{d}_v^{(14)},$$

$$\hat{d}_v^{(7)} = \Phi_v^{(4)} - \hat{d}_v^{(11)} - \hat{d}_v^{(13)} - \hat{d}_v^{(14)}.$$

The following theorem presents the errors of the above estimates  $\hat{d}_v^{(1)}, \dots, \hat{d}_v^{(14)}$  for any  $v$  in undirected graph  $G$ .

**THEOREM 10.** For  $i \in \{1, \dots, 14\}$ ,  $\hat{d}_v^{(i)}$  is an unbiased estimate of  $d_v^{(i)}$  with the following variance.

**(I)** For undirected orbit  $i \in \{1, \dots, 14\} \setminus \{2, 4, 7\}$ , the variance of  $\hat{d}_v^{(i)}$  is computed as

$$\text{Var}(\hat{d}_v^{(i)}) = \begin{cases} \frac{d_v^{(1)}}{K^{(3,2)}} \left( \frac{1}{p_1^{(3,2)}} - d_v^{(1)} \right), & i = 1, \\ \frac{d_v^{(i)}}{K^{(4,1)}} \left( \frac{1}{p_i^{(4,1)}} - d_v^{(i)} \right), & i \in \{5, 8, 11\}, \\ \frac{d_v^{(i)}}{K^{(4,2)}} \left( \frac{1}{p_i^{(4,2)}} - d_v^{(i)} \right), & i \in \{6, 9\}, \\ \frac{\text{Var}(\tilde{d}_v^{(i)}) \text{Var}(\hat{d}_v^{(i)})}{\text{Var}(\tilde{d}_v^{(i)}) + \text{Var}(\hat{d}_v^{(i)})}, & i \in \{3, 10, 12, 13, 14\}, \end{cases}$$

where  $\text{Var}(\tilde{d}_v^{(i)})$  and  $\text{Var}(\hat{d}_v^{(i)})$  are defined in Eqs. (5), (6), (8) and (9).

**(II)** For undirected orbit 2, the formula of  $\text{Var}(\hat{d}_v^{(2)})$  equals that of  $\text{Var}(\hat{d}_v^{(3)})$  derived above.

**(III)** For undirected orbit 4,  $\text{Var}(\hat{d}_v^{(4)})$  is computed as

$$\text{Var}(\hat{d}_v^{(4)}) = \sum_{j \in \{3, 8, 9, 10, 12, 13, 14\}} \chi_j^2 \text{Var}(\hat{d}_v^{(j)}) + \sum_{j, k \in \{3, 8, 9, 10, 12, 13, 14\} \wedge j \neq k} \chi_j \chi_k \text{Cov}(\hat{d}_v^{(j)}, \hat{d}_v^{(k)}), \quad (11)$$

where  $\chi_3 = \chi_8 = \chi_9 = \chi_{13} = 2$ ,  $\chi_{10} = 1$ ,  $\chi_{12} = 4$ , and  $\chi_{14} = 6$ .

**(IV)** For undirected orbit 7,  $\text{Var}(\hat{d}_v^{(7)})$  is computed as

$$\text{Var}(\hat{d}_v^{(7)}) = \text{Var}(\hat{d}_v^{(11)}) + \text{Var}(\hat{d}_v^{(13)}) + \text{Var}(\hat{d}_v^{(14)}) + \sum_{j, l \in \{11, 13, 14\} \wedge j \neq l} \text{Cov}(\hat{d}_v^{(j)}, \hat{d}_v^{(l)}). \quad (12)$$

The covariances in the formulas of  $\text{Var}(\hat{d}_v^{(4)})$  and  $\text{Var}(\hat{d}_v^{(7)})$  (i.e., Eqs. (11) and (12)) are computed as:

1. When  $j, l \in \{5, 8, 11\}$  and  $j \neq l$ ,  $\text{Cov}(\hat{d}_v^{(j)}, \hat{d}_v^{(l)}) = -\frac{d_v^{(j)} d_v^{(l)}}{K^{(4,1)}}$ ;
2. When  $j \in \{5, 8, 11\}$ ,  $\text{Cov}(\hat{d}_v^{(j)}, \hat{d}_v^{(3)}) = \text{Cov}(\hat{d}_v^{(3)}, \hat{d}_v^{(j)}) = -\frac{\lambda_v^{(3,1)} d_v^{(3)} d_v^{(j)}}{K^{(4,1)}}$ ;
3. When  $j, l \in \{6, 9\}$  and  $j \neq l$ ,  $\text{Cov}(\hat{d}_v^{(j)}, \hat{d}_v^{(l)}) = -\frac{d_v^{(j)} d_v^{(l)}}{K^{(4,2)}}$ ;
4. When  $j, l \in \{10, 12, 13, 14\}$  and  $j \neq l$ , we have  $\text{Cov}(\hat{d}_v^{(j)}, \hat{d}_v^{(l)}) = -\frac{\lambda_v^{(j,1)} \lambda_v^{(l,1)} d_v^{(j)} d_v^{(l)}}{K^{(4,1)}} - \frac{\lambda_v^{(j,2)} \lambda_v^{(l,2)} d_v^{(j)} d_v^{(l)}}{K^{(4,2)}}$ ;
5. When  $j \in \{3, 5, 8, 11\}$  and  $l \in \{6, 9\}$ , we have  $\text{Cov}(\hat{d}_v^{(j)}, \hat{d}_v^{(l)}) = \text{Cov}(\hat{d}_v^{(l)}, \hat{d}_v^{(j)}) = 0$ ;
6. When  $j \in \{5, 8, 11\}$  and  $l \in \{10, 12, 13, 14\}$ ,  $\text{Cov}(\hat{d}_v^{(j)}, \hat{d}_v^{(l)}) = \text{Cov}(\hat{d}_v^{(l)}, \hat{d}_v^{(j)}) = -\frac{\lambda_v^{(l,1)} d_v^{(j)} d_v^{(l)}}{K^{(4,1)}}$ ;
7. When  $j \in \{6, 9\}$  and  $l \in \{10, 12, 13, 14\}$ ,  $\text{Cov}(\hat{d}_v^{(j)}, \hat{d}_v^{(l)}) = \text{Cov}(\hat{d}_v^{(l)}, \hat{d}_v^{(j)}) = -\frac{\lambda_v^{(l,2)} d_v^{(j)} d_v^{(l)}}{K^{(4,2)}}$ ;
8. When  $j \in \{10, 12, 13, 14\}$ ,  $\text{Cov}(\hat{d}_v^{(3)}, \hat{d}_v^{(j)}) = \text{Cov}(\hat{d}_v^{(j)}, \hat{d}_v^{(3)}) = -\frac{\lambda_v^{(3,1)} \lambda_v^{(j,1)} d_v^{(3)} d_v^{(j)}}{K^{(4,1)}}$ .

## 6. SAND-3D: ESTIMATION OF DIRECTED ORBIT DEGREES

Due to a large number of directed 4-node graphlets and orbits, in this paper we focus on 3-node directed graphlets and orbits. Next, we introduce our method for estimating 3-node directed orbit degrees.

### 6.1 Estimating Single Directed Orbit Degree

For a directed orbit  $i$ , denote  $unorbit(i)$  as its associated undirected orbit when discarding the directions of edges in the graphlet. For example, directed orbits 2, 4, 5, 7, 9, 10, 12, 13, and 15 in Fig. 1(b) are associated with undirected orbit 1 in Fig. 1(a), directed orbits 1, 3, 6, 8, 11, and 14 in Fig. 1(b) are associated with undirected orbit 2 in Fig. 1(a), and directed orbits 16–30 in Fig. 1(b) are associated with undirected orbit 3 in Fig. 1(a). Given a sampling method from Section 3, the probability of it sampling a CIS in directed orbit  $i$ , denoted by  $p_i$ , equals the probability of the method sampling undirected orbit  $unorbit(i)$  derived in Section 3. When undirected orbit  $unorbit(i)$  can only be sampled by one method in Section 3 (e.g., Randgraf-3-2 is the only one that can sample  $unorbit(i) = 1$ ), we use the method to obtain  $K$  CISes that include a node  $v \in V$ . Let  $m_i$  denote the number of sampled CISes that include  $v$  in directed orbit  $i$ . According to Theorem 1, we estimate  $d_v^{(i,dir)}$  as

$$\hat{d}_v^{(i,dir)} = \frac{m_i}{K p_i}$$

with variance  $\text{Var}(\hat{d}_v^{(i,dir)}) = \frac{d_v^{(i,dir)}}{K} \left( \frac{1}{p_i} - d_v^{(i,dir)} \right)$ . When more than one method is able to sample undirected orbit  $unorbit(i)$ , we select the most efficient method, the one with the smallest  $\frac{\text{Var}(\hat{d}_v^{(i,dir)})}{K t_v}$  to estimate  $d_v^{(i,dir)}$ , where  $t_v$  is the average computational time of the method sampling a CIS, which is shown in Table 2.

### 6.2 Estimating all Directed Orbit Degrees

We develop method SAND-3D consisting of both Randgraf-3-1 and Randgraf-3-2 to estimate all 3-node directed orbit degrees  $d_v^{(1,dir)}, \dots, d_v^{(30,dir)}$ . Directed orbit  $i \in \{1, 3, 6, 8, 11, 14\}$  can be sampled by Randgraf-3-1 but not Randgraf-3-2, so we compute  $d_v^{(i,dir)}$  as the unbiased estimate given by Randgraf-3-1. Di-

rected orbit  $i \in \{2, 4, 5, 7, 9, 10, 12, 13, 15\}$  can be sampled by Randgraf-3-2 but not Randgraf-3-1, so we compute  $d_v^{(i,dir)}$  as the unbiased estimate given by Randgraf-3-2. We estimate  $d_v^{(i,dir)}$  for directed orbit  $i \in \{16, 17, \dots, 30\}$ , by combining two unbiased estimates given by Randgraf-3-1 and Randgraf-3-2 according to Theorem 2.

## 7. EVALUATION

### 7.1 Datasets

We perform our experiments on the following publicly available datasets taken from the Stanford Network Analysis Platform (SNAP)<sup>3</sup>, which are summarized in Table 3. We evaluate our method for computing the orbit degrees of node  $v_{\max}$  with the largest degree in the graph of interest.

**Table 3: Graph datasets used in our experiments. "edges" refers to the number of edges in the undirected graph generated by discarding edge directions. "max-degree" represents the maximum number of edges incident to a node in the undirected graph.**

graph	nodes	edges	max-degree
Flickr [14]	1,715,255	15,555,041	27,236
Pokec [15]	1,632,803	22,301,964	14,854
LiveJournal [14]	5,189,809	48,688,097	15,017
YouTube [14]	1,138,499	2,990,443	28,754
Wiki-Talk [12]	2,394,385	4,659,565	100,029
Web-Google [16]	875,713	4,322,051	6,332

### 7.2 Metric

We use the normalized root mean square error (NRMSE) to measure the relative error of the orbit degree estimate  $\hat{d}_{v_{\max}}^{(i)}$  with respect to its true value  $d_{v_{\max}}^{(i)}$ ,  $i = 1, 2, \dots$ . It is defined as:

$$\text{NRMSE}(\hat{d}_{v_{\max}}^{(i)}) = \frac{\sqrt{\text{MSE}(\hat{d}_{v_{\max}}^{(i)})}}{d_{v_{\max}}^{(i)}}, \quad i = 1, 2, \dots,$$

where  $\text{MSE}(\hat{d}_{v_{\max}}^{(i)})$  denotes the mean square error of  $\hat{d}_{v_{\max}}^{(i)}$ :

$$\begin{aligned} \text{MSE}(\hat{d}_{v_{\max}}^{(i)}) &= \mathbb{E}((\hat{d}_{v_{\max}}^{(i)} - d_{v_{\max}}^{(i)})^2) \\ &= \text{Var}(\hat{d}_{v_{\max}}^{(i)}) + \left( \mathbb{E}(\hat{d}_{v_{\max}}^{(i)}) - d_{v_{\max}}^{(i)} \right)^2. \end{aligned}$$

$\text{MSE}(\hat{d}_{v_{\max}}^{(i)})$  decomposes into a sum of the variance and bias of the estimator  $\hat{d}_{v_{\max}}^{(i)}$ , both quantities are important and need to be as small as possible to achieve good estimation performance. When  $\hat{d}_{v_{\max}}^{(i)}$  is an unbiased estimator of  $d_{v_{\max}}^{(i)}$ , we have  $\text{MSE}(\hat{d}_{v_{\max}}^{(i)}) = \text{Var}(\hat{d}_{v_{\max}}^{(i)})$ . In our experiments, we average the estimates and calculate their NRMSEs over 1,000 runs. We evenly distribute the sampling budget among the sampling methods of SAND and SAND-3D, and leave the optimal budget distribution in future study. Our experiments are conducted on a server with a Quad-Core AMD Opteron (tm) 8379 HE CPU 2.39 GHz processor and 128 GB DRAM memory.

### 7.3 Results

<sup>3</sup>www.snap.stanford.edu

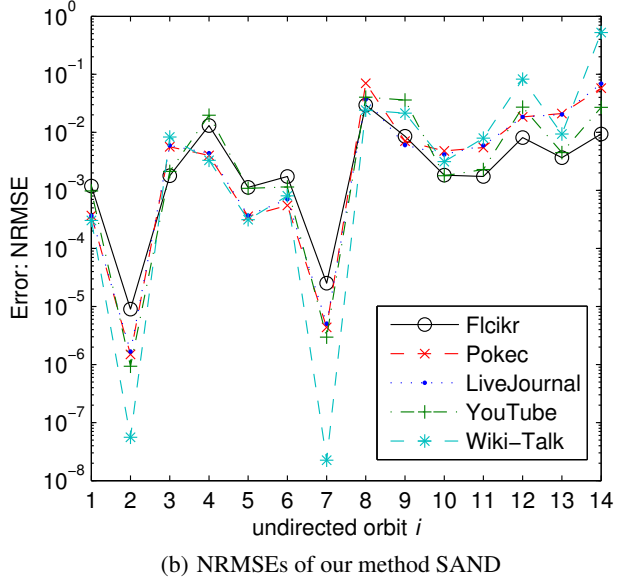
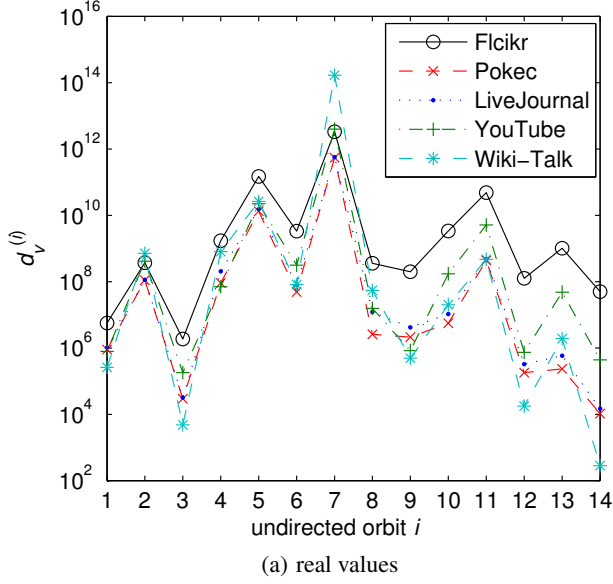


Figure 4: Real values and NRMSEs of our estimates of 3- and 4-node undirected orbit degrees of node  $v_{\max}$ .

### 7.3.1 Estimating undirected orbit degrees

We evaluate the performance of SAND by comparing its performance to the state-of-the-art enumeration method 4-Prof-Dist [17] for estimating 3- and 4-node undirected orbit degrees over the undirected graphs of datasets Flickr, Pokec, LiveJournal, YouTube, and Wiki-Talk, which are obtained by discarding edge directions. Table 4 shows that with a sampling budget  $10^6$  SAND is 183, 3.9, 15, and 81 times faster than 4-Prof-Dist for computing 3- and 4-node undirected orbit degrees of graphs Flickr, Pokec, LiveJournal, YouTube, and Wiki-Talk respectively. Fig. 4(a) shows the real values of 3- and 4-node undirected orbit degrees of  $v_{\max}$ . Roughly speaking, 3- and 4-node undirected orbit degree distributions of graphs Flickr, Pokec, LiveJournal, YouTube, and Wiki-Talk exhibit similar patterns.  $d_{v_{\max}}^{(7)}$ ,  $d_{v_{\max}}^{(5)}$ , and  $d_{v_{\max}}^{(11)}$  are the three largest 3- and 4-node undirected orbit degrees. Fig. 4(b) shows the NRMSEs of our estimates  $\hat{d}_{v_{\max}}^{(i)}$ ,  $i = 1, \dots, 14$ . We observe that all NRMSEs of  $\hat{d}_{v_{\max}}^{(i)}$  are smaller than 0.1 except the NRMSE of  $\hat{d}_{v_{\max}}^{(14)}$ . The NRMSEs of Top-3 orbits degrees  $\hat{d}_{v_{\max}}^{(7)}$ ,  $\hat{d}_{v_{\max}}^{(5)}$ , and  $\hat{d}_{v_{\max}}^{(11)}$  are smaller than 0.01.

Table 4: Computational cost of computing 3- and 4-node undirected orbit degrees of node  $v_{\max}$ .

graph	computational time (seconds)	
	4-Prof-Dist [17]	SAND
Flickr	7,681	41.9
Pokec	179	45.7
LiveJournal	300	58.2
YouTube	675	45.3
Wiki-Talk	3,489	43.0

### 7.3.2 Estimating directed orbit degrees

To the best of our knowledge, there exist no sampling method for estimating 3-node directed orbit degrees. Therefore, we evalu-

ate the performance of SAND-3D in comparison with the method of enumerating and classifying all the 3-node CISEs that include  $v_{\max}$ . Table 5 shows that with a sampling budget  $10^6$  SAND-3D is 229, 76.1, 246, 36,034 and 12.7 times faster than the enumeration method for computing 3-node directed orbit degrees of graphs Flickr, Pokec, LiveJournal, YouTube, Wiki-Talk, and Web-Google respectively. Let  $\frac{\hat{d}_{v_{\max}}^{(i, \text{dir})}}{\sum_{j=1}^{30} \hat{d}_{v_{\max}}^{(j, \text{dir})}} \times 100\%$  denote the normalized 3-node directed orbit  $i$  degrees of  $v_{\max}$ ,  $1 \leq i \leq 30$ . Fig. 5 shows the real values of normalized 3-node directed orbit degrees of  $v_{\max}$ . We observe that the 3-node directed orbit degrees of  $v_{\max}$  exhibit quite different patterns for different graphs. For example, Flickr and Wiki-Talk have the largest graphlet degree in directed orbit 1, Pokec and Web-Google have the largest graphlet degree in directed orbit 6, LiveJournal has the largest graphlet degree in directed orbit 14, and YouTube has the largest graphlet degree in directed orbit 11. Fig. 6 shows the NRMSEs of our estimates  $\hat{d}_{v_{\max}}^{(i, \text{dir})}$ ,  $i = 1, \dots, 30$ . We observe that the NRMSEs of estimates of the ten largest orbit degrees are smaller than 0.1 for all the graphs studied in this paper.

Although the NRMSEs of small orbit degrees exhibit large errors, we observe that SAND-3D is accurate enough for applications such as detecting the most frequent orbits, i.e., the orbits with the largest orbit degrees. Table 6 shows the results of detecting the five, ten, and fifteen most frequent directed orbits. We can see that SAND-3D successfully identifies all the five and ten most frequent directed orbits. On average, no more than one of the fifteen most frequent directed orbits is missed by SAND-3D. We also study the  $L_1$  and  $L_2$  distances between our estimates and real values, which are defined as  $L_1 = \sum_{i=1}^{30} \left| \frac{\hat{d}_{v_{\max}}^{(i, \text{dir})}}{\sum_{j=1}^{30} \hat{d}_{v_{\max}}^{(j, \text{dir})}} - \frac{d_{v_{\max}}^{(i, \text{dir})}}{\sum_{j=1}^{30} d_{v_{\max}}^{(j, \text{dir})}} \right|$  and

$$L_2 = \sum_{i=1}^{30} \sqrt{\left( \frac{\hat{d}_{v_{\max}}^{(i, \text{dir})}}{\sum_{j=1}^{30} \hat{d}_{v_{\max}}^{(j, \text{dir})}} - \frac{d_{v_{\max}}^{(i, \text{dir})}}{\sum_{j=1}^{30} d_{v_{\max}}^{(j, \text{dir})}} \right)^2}.$$

Table 7 shows that  $L_1$  and  $L_2$  distances are smaller than 0.001 and 0.002 respectively. This indicates that estimates given by SAND-3D are accurate for  $L_1$  and  $L_2$  distances based machine learning applications.

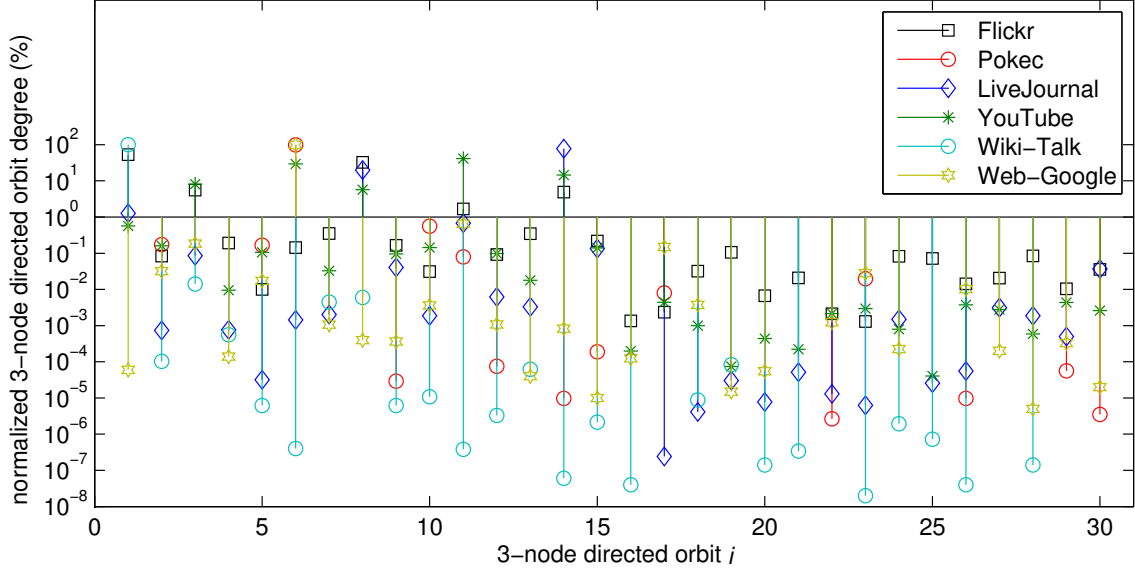


Figure 5: Real values of normalized 3-node directed orbit degrees of node  $v_{\max}$ , i.e.,  $\frac{d_{v_{\max}}^{(i, \text{dir})}}{\sum_{j=1}^{30} d_{v_{\max}}^{(j, \text{dir})}} \times 100\%$ ,  $1 \leq i \leq 30$ .

Table 5: Computational cost of computing 3-node directed orbit degrees of node  $v_{\max}$ .

graph	computational time (seconds)	
	enumeration method	SAND-3D
Flickr	1,461	6.38
Pokec	367	4.82
LiveJournal	472	6.69
YouTube	1,294	5.26
Wiki-Talk	181,609	5.04
Web-Google	61.7	4.87

Table 6: Accuracy of identifying the five, ten, and fifteen most frequent 3-node directed orbits of  $v_{\max}$ .

graph	# Top frequent orbits correctly detected		
	Top-5	Top-10	Top-15
Flickr	5	10	14.9
Pokec	5	10	15.0
LiveJournal	5	10	14.0
YouTube	5	10	14.5
Wiki-Talk	5	10	15.0
Web-Google	5	10	14.6

## 8. RELATED WORK

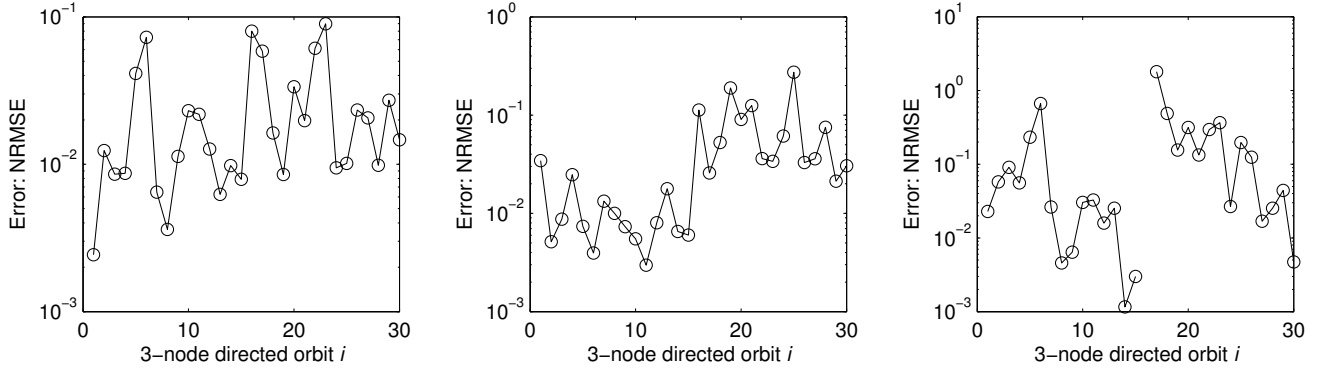
Recently, a number of efforts have focused on designing sampling methods for computing a large graph’s graphlet concentrations [18–24] and graphlet counts [7–11, 18]. To estimate graphlet concentrations, Kashtan et al. [19] proposed a simple subgraph sampling method. However their method is computationally expensive when calculating the weight of each sampled subgraph, which is used for correcting bias introduced by edge sampling. To address this drawback, Wernicke [20] proposed a method named FANMOD based on enumerating subgraph trees. GUISE proposed a Metropolis-Hastings based sampling method to estimate 3-node, 4-node, and 5-node graphlet concentrations<sup>4</sup>. These methods assume the entire topology of the graph of interest is known in advance and it can be fit into the memory. Wang et al. [24] propose an efficient crawling method to estimate online social network motif concentrations, when the graph’s topology is not available in advance and it is costly to sample the entire topology. When the available dataset is a set of random edges sampled from streaming

<sup>4</sup>The concentration of a particular  $k$ -node graphlet in a network refers to the ratio of the graphlet count to the total number of  $k$ -node CISes in the network,  $k = 3, 4, 5, \dots$

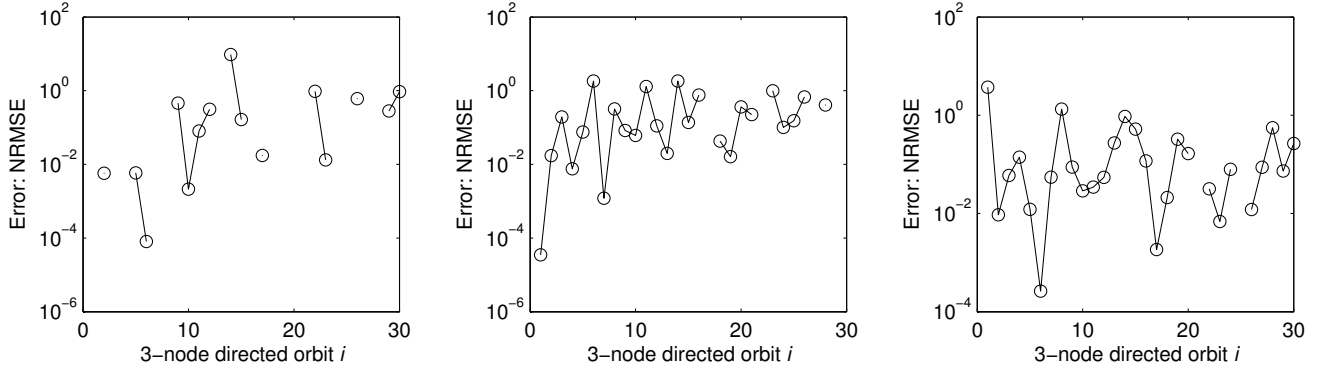
graphs<sup>5</sup>, Wang et al. [25] propose an efficient crawling method to estimate graphlet concentrations.

The above methods fail to compute graphlet counts, which is more fundamental than graphlet concentrations. Alon et al. [18] propose a color-coding method to reduce the computational cost of counting subgraphs. Color-coding reduces computation by coloring nodes randomly and enumerating only colorful CISes (i.e., CISes that consist of nodes with distinct colors), but [11] reveals that the color-coding method is not scalable and is hindered by the sheer number of colorful CISes. [7–10] develop sampling methods to estimate the number of triangles of static and dynamic graphs. Jha et al. [11] develop sampling methods to estimate counts of 4-node undirected graphlets. Wang et al. [26] develop a sampling method to estimate counts of 5-node undirected motifs. These methods are designed to sample all subgraphs, but not tailored to meet the need of sampling the subgraphs **that include a given node**. Elenberg et al. [17] develop a method to estimate counts of 4-node undirected motifs that include a given node based on random edge sampling, but their sampling method cannot be used to estimate node orbit degrees because the orbit of a node in a sampled CIS may be different from that of the node in the original CISes.

<sup>5</sup>Streaming graph is given in form of a stream of edges.



(a) Flickr. Top-10 directed orbits with the (b) Pokec. Top-10 directed orbits with the (c) YouTube. Top-10 directed orbits with the largest orbit degrees: 1, 8, 3, 14, 11, 7, 13, largest orbit degrees: 11, 6, 14, 3, 8, 1, 2, 10, largest orbit degrees: 14, 8, 1, 11, 15, 3, 9, 30, 15, 4, and 9. 15, and 5. 12, and 13.



(d) LiveJournal. Top-10 directed orbits with (e) Wiki-Talk. Top-10 directed orbits with the (f) Web-Google. Top-10 directed orbits with the largest orbit degrees: 6, 10, 2, 5, 11, 23, largest orbit degrees: 1, 3, 8, 7, 4, 2, 19, 13, the largest orbit degrees: 6, 11, 3, 17, 2, 23, 5, 17, 15, 12, and 29. 10, and 18. 26, 18, and 10.

**Figure 6: NRMSEs of our estimates of 3-node directed orbit degrees.**

**Table 7: Errors**  $L_2 = \sum_{i=1}^{30} \sqrt{\left( \frac{\hat{d}_{v_{\max}}^{(i, \text{dir})}}{\sum_{j=1}^{30} \hat{d}_{v_{\max}}^{(j, \text{dir})}} - \frac{d_{v_{\max}}^{(i, \text{dir})}}{\sum_{j=1}^{30} d_{v_{\max}}^{(j, \text{dir})}} \right)^2}$

and  $L_1 = \sum_{i=1}^{30} \left| \frac{\hat{d}_{v_{\max}}^{(i, \text{dir})}}{\sum_{j=1}^{30} \hat{d}_{v_{\max}}^{(j, \text{dir})}} - \frac{d_{v_{\max}}^{(i, \text{dir})}}{\sum_{j=1}^{30} d_{v_{\max}}^{(j, \text{dir})}} \right|$ .

graph	$L_2$		$L_1$	
	mean	variance	mean	variance
Flickr	9.1e-04	2.5e-07	1.8e-03	7.1e-07
Pokec	1.1e-03	1.8e-07	2.1e-03	5.9e-07
LiveJournal	4.1e-05	9.0e-10	7.0e-05	2.1e-09
YouTube	6.2e-04	1.5e-07	1.1e-03	3.5e-07
Wiki-Talk	2.3e-05	1.7e-10	3.6e-05	4.1e-10
Web-Google	1.6e-04	9.6e-09	2.6e-04	2.3e-08

We point out that method 4-Prof-Dist in [17] can be easily extended and used to compute the exact values of a node’s 4-node undirected orbit degrees, but it fails to compute directed orbit degrees. To the best of our knowledge, we are the first to propose sampling methods for estimating a node’s orbit degrees for large graphs.

## 9. CONCLUSIONS AND FUTURE WORK

We develop computationally efficient sampling methods to esti-

mate the counts of 3- and 4-node undirected and directed graphlet orbit degrees for large graphs. We provide unbiased estimators of graphlet orbit degrees, and derive simple and exact formulas for the variances of the estimators. Meanwhile, we conduct experiments on a variety of publicly available datasets, and experimental results show that our methods accurately estimates graphlet orbit degrees for the nodes with the largest degrees in graphs with millions of edges within one minute. In future, we plan to extend SAND to estimate 5-node (or even higher order) graphlet orbit degrees and investigate the graphlet orbit degree signatures as features for various learning tasks.

## Acknowledgment

This work was supported in part by ARL under Cooperative Agreement W911NF-09-2-0053. The views and conclusions contained in this document are those of the authors and should not be interpreted as representing the official policies, either expressed or implied of the ARL, or the U.S. Government. This work was supported in part by the National Natural Science Foundation of China (61103240, 61103241, 61221063, 61221063, 91118005, U1301254), the 111 International Collaboration Program of China, 863 High Tech Development Plan (2012AA011003), the Prospective Research Project on Future Networks of Jiangsu Future Networks Innovation Institute, and the Application Foundation Research Program of Suzhou

(SYG201311). The work of John C.S. Lui was supported in part by the GRF 415013.

## Appendix

### Implementation Details

We discuss our methods for implementing the functions in the Algorithms we presented subsections 4.1 and 4.2. We also analyze their computational complexities.

**Initialization of  $\phi_v, \varphi_v, \Phi_v^{(1)}, \Phi_v^{(2)}, \Phi_v^{(3)}$ , and  $\Phi_v^{(4)}$ :** For each node  $v$ , we store its degree  $d_v$  and store its neighbors' degrees in a list. Therefore,  $O(1)$  and  $O(d_v)$  operations are required to compute  $\phi_v$  and  $\varphi_v$  respectively. Similarly, one can easily find that  $O(N_v), O(N_v), O(\sum_{u \in N_v} d_u)$ , and  $O(1)$  operations are required to compute  $\Phi_v^{(1)}, \Phi_v^{(2)}, \Phi_v^{(3)}$ , and  $\Phi_v^{(4)}$  respectively.

**RandomVertex( $N_v$ ):** We use an array  $N_v[1, \dots, d_v]$  to store the neighbors of  $v$ . Function  $\text{RandomVertex}(N_v \setminus \{u\})$  first randomly selects number  $rnd$  from  $\{1, \dots, d_v\}$  and then returns node  $N_v[rnd]$ . Its computational complexity is just  $O(1)$ .

**RandomVertex( $N_v \setminus \{u\}$ ):** Let  $POS_{v,u}$  denote the index of  $u$  in the list  $N_v[1, \dots, d_v]$ , i.e.,  $N_v[POS_{v,u}] = u$ . Then, function  $\text{RandomVertex}(N_v \setminus \{u\})$  includes the following steps:

- **Step 1:** Select number  $rnd$  from  $\{1, \dots, d_v\} \setminus \{POS_{v,u}\}$  at random;
- **Step 2:** Return  $N_v[rnd]$ .

Its computational complexity is  $O(1)$ .

**RandomVertex( $N_v \setminus \{u, w\}$ ):** Similarly,  $\text{RandomVertex}(N_v \setminus \{u, w\})$  includes the following steps:

- **Step 1:** Select number  $rnd$  from  $\{1, \dots, d_v\} \setminus \{POS_{v,u}, POS_{v,w}\}$  at random;
- **Step 2:** Return  $N_v[rnd]$ .

Its computational complexity is  $O(1)$ .

**WeightRandomVertex( $N_v, \alpha^{(v)}$ ):** We store an array  $ACC_{-\alpha^{(v)}}$  in memory, where  $ACC_{-\alpha^{(v)}}[i]$  is defined as  $ACC_{-\alpha^{(v)}}[i] = \sum_{j=1}^i (d_{N_v[j]} - 1)$ ,  $1 \leq i \leq d_v$ . Let  $ACC_{-\alpha^{(v)}}[0] = 0$ . Then,  $\text{WeightRandomVertex}(N_v, \alpha^{(v)})$  includes the following steps:

- **Step 1:** Select number  $rnd$  from  $\{1, \dots, ACC_{-\alpha^{(v)}}[d_v]\}$  at random;
- **Step 2:** Find  $i$  such that

$$ACC_{-\alpha^{(v)}}[i-1] < rnd \leq ACC_{-\alpha^{(v)}}[i],$$

which is solved by binary search;

- **Step 3:** Return  $N_v[i]$ .

Its computational complexity is  $O(\log d_v)$ .

**WeightRandomVertex( $N_v, \beta^{(v)}$ ):** We store an array  $ACC_{-\beta^{(v)}}$  in memory, where  $ACC_{-\beta^{(v)}}[i]$  is defined as  $ACC_{-\beta^{(v)}}[i] = \sum_{j=1}^i (\phi_{N_v[j]} - d_{N_v[j]} + 1)$ ,  $1 \leq i \leq d_v$ . Let  $ACC_{-\beta^{(v)}}[0] = 0$ . Then,  $\text{WeightRandomVertex}(N_v, \beta^{(v)})$  includes the following steps:

- **Step 1:** Select number  $rnd$  from  $\{1, \dots, ACC_{-\beta^{(v)}}[d_v]\}$  at random;
- **Step 2:** Find  $i$  such that

$$ACC_{-\beta^{(v)}}[i-1] < rnd \leq ACC_{-\beta^{(v)}}[i],$$

which again is solved by binary search;

- **Step 3:** Return  $N_v[i]$ .

Its computational complexity is  $O(\log d_v)$ .

**WeightRandomVertex( $N_v, \gamma^{(v)}$ ):** We store an array  $ACC_{-\gamma^{(v)}}$  in memory, where  $ACC_{-\gamma^{(v)}}[i]$  is defined as  $ACC_{-\gamma^{(v)}}[i] = \sum_{j=1}^i (\varphi_{N_v[j]} - d_v + 1)$ ,  $1 \leq i \leq d_v$ . Let  $ACC_{-\gamma^{(v)}}[0] = 0$ . Then,  $\text{WeightRandomVertex}(N_v, \gamma^{(v)})$  includes the following steps:

- **Step 1:** Select number  $rnd$  from  $\{1, \dots, ACC_{-\gamma^{(v)}}[d_v]\}$  at random;

- **Step 2:** Find  $i$  such that

$$ACC_{-\gamma^{(v)}}[i-1] < rnd \leq ACC_{-\gamma^{(v)}}[i],$$

which again is solved by binary search;

- **Step 3:** Return  $N_v[i]$ .

Its computational complexity is  $O(\log d_v)$ .

**WeightRandomVertex( $N_u \setminus \{v\}, \rho^{(u,v)}$ ):** As alluded, we use  $N_u[1, \dots, d_u]$  to store the neighbors of  $u$ , and  $ACC_{-\alpha^{(u)}}[1, \dots, d_u]$  to store  $ACC_{-\alpha^{(u)}}[i] = \sum_{j=1}^i (d_{N_u[j]} - 1)$ ,  $1 \leq i \leq d_u$ . Let  $POS_{u,v}$  be the index of  $v$  in  $N_u[1, \dots, d_u]$ , i.e.,  $N_u[POS_{u,v}] = v$ . Then, function  $\text{WeightRandomVertex}(N_u \setminus \{v\}, \rho^{(u,v)})$  consists of the following steps:

- **Step 1:** Select number  $rnd$  from  $\{1, \dots, ACC_{-\alpha^{(u)}}[d_u]\} \setminus \{ACC_{-\alpha^{(u)}}[POS_{u,v}-1] + 1, \dots, ACC_{-\alpha^{(u)}}[POS_{u,v}]\}$  at random;

- **Step 2:** Find  $i$  such that

$$ACC_{-\alpha^{(u)}}[i-1] < rnd \leq ACC_{-\alpha^{(u)}}[i],$$

which is solved by binary search;

- **Step 3:** Return  $N_u[i]$ .

Its computational complexity is  $O(\log d_u)$ .

### Proof of Theorem 1

For  $1 \leq i \leq r$  and  $1 \leq j \leq K$ , we have

$$P(X_j \in S_i) = \sum_{s \in S_i} P(X_j = s, s \in S_i) = p_i n_i.$$

Since  $X_1, \dots, X_K$  are sampled independently, the random variable  $\sum_{j=1}^K \mathbf{1}(X_j \in S_i)$  follows the binomial distribution with parameters  $K$  and  $p_i n_i$ . Then, the expectation and variance of  $\sum_{j=1}^K \mathbf{1}(X_j \in S_i)$  are

$$\mathbb{E} \left( \sum_{j=1}^K \mathbf{1}(X_j \in S_i) \right) = K p_i n_i,$$

$$\text{Var} \left( \sum_{j=1}^K \mathbf{1}(X_j \in S_i) \right) = K p_i n_i (1 - p_i n_i).$$

Therefore, the expectation and variance of  $\hat{n}_i$  are computed as

$$\mathbb{E}(\hat{n}_i) = \mathbb{E} \left( \frac{\sum_{j=1}^K \mathbf{1}(X_j \in S_i)}{K p_i} \right) = n_i,$$

$$\text{Var}(\hat{n}_i) = \text{Var} \left( \frac{\sum_{j=1}^K \mathbf{1}(X_j \in S_i)}{K p_i} \right) = \frac{n_i}{K} \left( \frac{1}{p_i} - n_i \right).$$

For  $i \neq j$  and  $1 \leq i, j \leq r$ , the covariance of  $\hat{n}_i$  and  $\hat{n}_j$  is

$$\begin{aligned}
& \text{Cov}(\hat{n}_i, \hat{n}_j) \\
&= \text{Cov} \left( \frac{\sum_{t=1}^K \mathbf{1}(X_t \in S_i)}{K p_i}, \frac{\sum_{l=1}^K \mathbf{1}(X_l \in S_j)}{K p_j} \right) \\
&= \frac{\text{Cov}(\sum_{t=1}^K \mathbf{1}(X_t \in S_i), \sum_{l=1}^K \mathbf{1}(X_l \in S_j))}{K^2 p_i p_j} \\
&= \frac{\sum_{t=1}^K \sum_{l=1}^K \text{Cov}(\mathbf{1}(X_t \in S_i), \mathbf{1}(X_l \in S_j))}{K^2 p_i p_j} \\
&= \frac{\sum_{t=1}^K \text{Cov}(\mathbf{1}(X_t \in S_i), \mathbf{1}(X_t \in S_j))}{K^2 p_i p_j} \\
&= -\frac{n_i n_j}{K}.
\end{aligned}$$

In the derivation above, we use

$$\text{Cov}(\mathbf{1}(X_t \in S_i), \mathbf{1}(X_l \in S_j)) = 0, \quad t \neq l,$$

$$\begin{aligned}
& \text{Cov}(\mathbf{1}(X_t \in S_i), \mathbf{1}(X_t \in S_j)) \\
&= \mathbb{E}(\mathbf{1}(X_t \in S_i) \mathbf{1}(X_t \in S_j)) - \mathbb{E}(\mathbf{1}(X_t \in S_i)) \mathbb{E}(\mathbf{1}(X_t \in S_j)) \\
&= 0 - p_i n_i p_j n_j \\
&= -p_i p_j n_i n_j.
\end{aligned}$$

### Proof of Theorem 3

The number of selections of variables  $u$  and  $w$  in Algorithm 1 is  $\binom{d_v}{2} \times 2! = 2\phi_v$ . For a CIS  $s$  consisting three nodes  $v, u_1$ , and  $u_2$ , when  $s$  includes  $v$  in orbit 2 or 3, Randgraf-3-1 has two ways to sample  $s$ : (1)  $u = u_1$  and  $w = u_2$ ; (2)  $u = u_2$  and  $w = u_1$ . Each happens with probability  $\frac{1}{d_v} \times \frac{1}{d_v-1} = \frac{1}{2\phi_v}$ . Otherwise, Randgraf-3-1 is not able to sample  $s$ . Therefore, we have  $p_1^{(3,1)} = 0, p_2^{(3,1)} = \frac{1}{\phi_v}$ , and  $p_3^{(3,1)} = \frac{1}{\phi_v}$ .

### Proof of Theorem 4

The number of selections of variables  $u$  and  $w$  in Algorithm 2 is  $\varphi_v = \sum_{u \in N_v} (d_u - 1)$ . For a CIS  $s$  including  $v$  in orbit 1, Randgraf-3-2 has only one way to sample  $s$ , which happens with probability  $\alpha_u^{(v)} \times \frac{1}{d_v-1} = \frac{1}{\varphi_v}$ . When  $s$  including  $v$  in orbit 3, similar to Randgraf-3-1, Randgraf-3-2 has two different ways to sample  $s$ , where each happens with probability  $\frac{1}{\varphi_v}$ . When  $s$  including  $v$  in orbit 2, Randgraf-3-2 is not able to sample it. Therefore, we have  $p_1^{(3,2)} = \frac{1}{\varphi_v}, p_2^{(3,2)} = 0$ , and  $p_3^{(3,2)} = \frac{2}{\varphi_v}$ .

### Proof of Theorem 5

The number of selections of variables  $u, w$ , and  $r$  in Algorithm 3 is  $(d_v - 1) \sum_{u \in N_v} (d_u - 1) = \Phi_v^{(1)}$ . As shown in Fig. 7, Randgraf-4-1 has 2, 1, 2, 1, 2, 4, and 6 ways to sample a 3- or 4-node CIS  $s$  including  $v$  in orbits 3, 5, 8, 10, 11, 12, 13, and 14 respectively. Each way happens with probability  $\alpha_u^{(v)} \times \frac{1}{d_u-1} \times \frac{1}{d_v-1} = \frac{1}{\Phi_v^{(1)}}$ .

When  $s$  includes  $v$  in the other orbits, Randgraf-4-1 cannot not sample  $s$ . Therefore, we have  $p_1^{(4,1)} = p_2^{(4,1)} = p_4^{(4,1)} = p_6^{(4,1)} = p_7^{(4,1)} = p_9^{(4,1)} = 0, p_3^{(4,1)} = \frac{2}{\Phi_v^{(1)}}, p_5^{(4,1)} = \frac{1}{\Phi_v^{(1)}}, p_8^{(4,1)} = \frac{2}{\Phi_v^{(1)}}, p_{10}^{(4,1)} = \frac{1}{\Phi_v^{(1)}}, p_{11}^{(4,1)} = \frac{2}{\Phi_v^{(1)}}, p_{12}^{(4,1)} = \frac{2}{\Phi_v^{(1)}}, p_{13}^{(4,1)} = \frac{4}{\Phi_v^{(1)}}$ , and  $p_{14}^{(4,1)} = \frac{6}{\Phi_v^{(1)}}$ .

### Proof of Theorem 6

The number of selections of variables  $u, w$ , and  $r$  in Algorithm 4 is  $\sum_{u \in N_v} (d_u - 1)(d_u - 2) = 2\Phi_v^{(2)}$ . As shown in Fig. 8, Randgraf-

4-2 has 2, 2, 2, 4, 2, and 6 ways to sample a 4-node CIS  $s$  including  $v$  in orbits 6, 9, 10, 12, 13, and 14 respectively. Each way happens with probability  $\beta_u^{(v)} \times \frac{1}{d_u-1} \times \frac{1}{d_v-2} = \frac{1}{2\Phi_v^{(2)}}$ . When  $s$  includes  $v$  in the other orbits, Randgraf-4-2 is not able to sample  $s$ . Therefore, we have  $p_1^{(4,2)} = p_2^{(4,2)} = p_3^{(4,2)} = p_4^{(4,2)} = p_5^{(4,2)} = p_7^{(4,2)} = p_8^{(4,2)} = p_{11}^{(4,2)} = 0, p_6^{(4,2)} = \frac{1}{\Phi_v^{(2)}}, p_9^{(4,2)} = \frac{1}{\Phi_v^{(2)}}, p_{10}^{(4,2)} = \frac{1}{\Phi_v^{(2)}}, p_{12}^{(4,2)} = \frac{2}{\Phi_v^{(2)}}, p_{13}^{(4,2)} = \frac{1}{\Phi_v^{(2)}}$ , and  $p_{14}^{(4,2)} = \frac{3}{\Phi_v^{(2)}}$ .

### Proof of Theorem 7

The number of selections of variables  $u, w$ , and  $r$  in Algorithm 5 is  $\sum_{u \in N_v} \sum_{w \in N_u - \{v\}} (d_w - 1) = \sum_{u \in N_v} (\varphi_u - d_v + 1) = \Phi_v^{(3)}$ . As shown in Fig. 9, Randgraf-4-3 has 2, 1, 2, 2, 1, 4, 2, and 6 ways to sample a 4-node CIS  $s$  including  $v$  in orbits 3, 4, 8, 9, 10, 12, 13, and 14 respectively. Each way happens with probability  $\gamma_u^{(v)} \times \rho_u^{(u,v)} \times \frac{1}{d_w-1} = \frac{1}{\Phi_v^{(3)}}$ . When  $s$  includes  $v$  in the other orbits, Randgraf-4-3 is not able to sample  $s$ . Therefore, we have  $p_1^{(4,3)} = p_2^{(4,3)} = p_5^{(4,3)} = p_6^{(4,3)} = p_7^{(4,3)} = p_{11}^{(4,3)} = 0, p_3^{(4,3)} = \frac{2}{\Phi_v^{(3)}}, p_4^{(4,3)} = \frac{1}{\Phi_v^{(3)}}, p_8^{(4,3)} = \frac{2}{\Phi_v^{(3)}}, p_9^{(4,3)} = \frac{2}{\Phi_v^{(3)}}, p_{10}^{(4,3)} = \frac{1}{\Phi_v^{(3)}}, p_{12}^{(4,3)} = \frac{4}{\Phi_v^{(3)}}, p_{13}^{(4,3)} = \frac{2}{\Phi_v^{(3)}}$ , and  $p_{14}^{(4,3)} = \frac{6}{\Phi_v^{(3)}}$ .

### Proof of Theorem 8

The number of selections of variables  $u, w$ , and  $r$  in Algorithm 6 is  $\binom{d_v}{3} \times 3! = 6\Phi_v^{(4)}$ . For a CIS  $s$  consisting four nodes  $v, u_1, u_2$ , and  $u_3$ , when  $s$  includes  $v$  in orbit 7, 11, 13, or 14, Randgraf-4-4 has six ways to sample  $s$ : (1)  $u = u_1, w = u_2, r = u_3$ ; (2)  $u = u_1, w = u_3, r = u_2$ ; (3)  $u = u_2, w = u_1, r = u_3$ ; (4)  $u = u_2, w = u_3, r = u_1$ ; (5)  $u = u_3, w = u_1, r = u_2$ ; (6)  $u = u_3, w = u_2, r = u_1$ . Each one happens with probability  $\frac{1}{d_v} \times \frac{1}{d_v-1} \times \frac{1}{d_v-2} = \frac{1}{6\Phi_v^{(4)}}$ . When  $s$  includes  $v$  in the other orbits,

Randgraf-4-4 is not able to sample  $s$ . Therefore, we have  $p_1^{(4,4)} = p_2^{(4,4)} = p_3^{(4,4)} = p_4^{(4,4)} = p_5^{(4,4)} = p_6^{(4,4)} = p_8^{(4,4)} = p_9^{(4,4)} = p_{10}^{(4,4)} = p_{12}^{(4,4)} = 0$ , and  $p_7^{(4,4)} = p_{11}^{(4,4)} = p_{13}^{(4,4)} = p_{14}^{(4,4)} = \frac{1}{\Phi_v^{(4)}}$ .

### Proof of Theorem 9

We easily find that the total number of selections of  $u$  and  $w$  in Algorithm Randgraf-3-1 is  $2\phi_v$ . From the proof of Theorem 3, we observe: (1) Randgraf-3-1 has two ways to sample CISes including  $v$  in both orbits 2 and 3; (2) Randgraf-3-1 is not able to sample the other CISes including  $v$ . Therefore, we have  $2d_v^{(2)} + 2d_v^{(3)} = 2\phi_v$ .

We find that the total number of selections of  $u, w$ , and  $r$  in Algorithm Randgraf-4-3 is  $\Phi_v^{(3)}$ . From the proof of Theorem 7, we observe: (1) Randgraf-4-3 has 2, 1, 2, 2, 1, 4, 2, and 6 way/ways to sample CISes including  $v$  in orbits 3, 4, 8, 9, 10, 12, 13, and 14 respectively; (2) Randgraf-4-3 is not able to sample the other CISes including  $v$ . Therefore, we have

$$\begin{aligned}
& 2d_v^{(3)} + d_v^{(4)} + 2d_v^{(8)} + 2d_v^{(9)} + d_v^{(10)} + 4d_v^{(12)} + 2d_v^{(13)} \\
& + 6d_v^{(14)} = \Phi_v^{(3)}.
\end{aligned}$$

We find that the total number of selections of  $u, w$ , and  $r$  in Algorithm Randgraf-4-4 is  $6\Phi_v^{(4)}$ . From the proof of Theorem 8, we observe that (1) Randgraf-4-4 has 6 ways to sample CISes including  $v$  in orbits 7, 11, 13, and 14 respectively; (2) Randgraf-4-4 is not able to sample the other CISes including  $v$ . Thus, we have

$$d_v^{(7)} + d_v^{(11)} + d_v^{(13)} + d_v^{(14)} = \Phi_v^{(4)}.$$

<p>3 case 1: <math>u=u_1, w=u_2, r=u_2</math> case 2: <math>u=u_2, w=u_1, r=u_1</math></p>	<p>5 case 1: <math>u=u_1, w=u_2, r=u_3</math> 4 case 2: <math>u=u_2, w=u_1, r=u_1</math></p>	<p>8 case 1: <math>u=u_1, w=u_2, r=u_3</math> case 2: <math>u=u_2, w=u_1, r=u_3</math></p>
<p>11 case 1: <math>u=u_1, w=u_3, r=u_2</math> 9 case 2: <math>u=u_2, w=u_1, r=u_1</math></p>	<p>11 case 1: <math>u=u_1, w=u_2, r=u_3</math> 9 case 2: <math>u=u_3, w=u_2, r=u_1</math></p>	<p>13 case 1: <math>u=u_1, w=u_2, r=u_3</math> 12 case 2: <math>u=u_2, w=u_1, r=u_3</math></p>
<p>13 case 1: <math>u=u_1, w=u_2, r=u_3</math> 12 case 2: <math>u=u_2, w=u_1, r=u_3</math> 12 case 3: <math>u=u_3, w=u_2, r=u_1</math> 12 case 4: <math>u=u_3, w=u_1, r=u_2</math></p>	<p>14 case 1: <math>u=u_1, w=u_2, r=u_3</math> case 2: <math>u=u_1, w=u_3, r=u_2</math> case 3: <math>u=u_2, w=u_1, r=u_3</math></p>	<p>case 4: <math>u=u_2, w=u_3, r=u_1</math> case 5: <math>u=u_3, w=u_1, r=u_2</math> case 6: <math>u=u_3, w=u_2, r=u_1</math></p>

**Figure 7: The ways of Randgraf-4-1 sampling a CIS that includes  $v$  in different orbits. Numbers in blue are orbit IDs.  $u, w,$  and  $r$  in red are the variables in Algorithm 3.**

<p>7 case 1: <math>u=u_1, w=u_2, r=u_3</math> 6 case 2: <math>u=u_1, w=u_3, r=u_2</math></p>	<p>11 case 1: <math>u=u_1, w=u_2, r=u_3</math> 9 case 2: <math>u=u_1, w=u_3, r=u_2</math></p>	<p>11 case 1: <math>u=u_1, w=u_2, r=u_3</math> 9 case 2: <math>u=u_1, w=u_3, r=u_2</math></p>
<p>13 case 1: <math>u=u_1, w=u_2, r=u_3</math> 12 case 2: <math>u=u_1, w=u_3, r=u_2</math></p>	<p>case 3: <math>u=u_2, w=u_1, r=u_3</math> case 4: <math>u=u_2, w=u_3, r=u_1</math></p>	<p>13 case 1: <math>u=u_3, w=u_1, r=u_2</math> 12 case 2: <math>u=u_3, w=u_2, r=u_1</math></p>
<p>14 case 1: <math>u=u_1, w=u_2, r=u_3</math> case 2: <math>u=u_1, w=u_3, r=u_2</math> case 3: <math>u=u_2, w=u_1, r=u_3</math></p>	<p>case 4: <math>u=u_2, w=u_3, r=u_1</math> case 5: <math>u=u_3, w=u_1, r=u_2</math> case 6: <math>u=u_3, w=u_2, r=u_1</math></p>	

**Figure 8: The ways of Randgraf-4-2 sampling a CIS that includes  $v$  in different orbits. Numbers in blue are orbit IDs.  $u, w,$  and  $r$  in red are the variables in Algorithm 4.**

### Proof of Theorem 10

According to Theorems 1 and 4, we have

$$\text{Var}(\hat{d}_v^{(1)}) = \frac{d_v^{(1)}}{K^{(3,2)}} \left( \frac{1}{p_1^{(3,2)}} - d_v^{(1)} \right).$$

According to Theorems 1 and 5, we have

$$\text{Var}(\hat{d}_v^{(i)}) = \frac{d_v^{(i)}}{K^{(4,1)}} \left( \frac{1}{p_i^{(4,1)}} - d_v^{(i)} \right), i \in \{5, 8, 11\}.$$

According to Theorems 1 and 6, we have

$$\text{Var}(\hat{d}_v^{(i)}) = \frac{d_v^{(i)}}{K^{(4,2)}} \left( \frac{1}{p_i^{(4,2)}} - d_v^{(i)} \right), i \in \{6, 9\},$$

By Theorem 2 and the definition of  $\hat{d}_v^{(3)}, \hat{d}_v^{(10)}, \hat{d}_v^{(12)}, \hat{d}_v^{(13)},$  and  $\hat{d}_v^{(14)}$  in Eqs. (7) and (10), we have

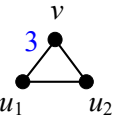
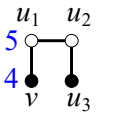
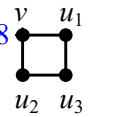
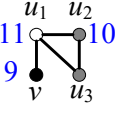
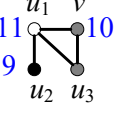
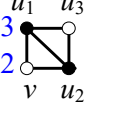
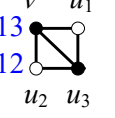
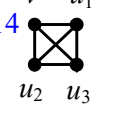
$$\begin{aligned} \text{Var}(\hat{d}_v^{(i)}) &= \text{Var} \left( \frac{\text{Var}(\tilde{d}_v^{(i)})\tilde{d}_v^{(i)} + \text{Var}(\check{d}_v^{(i)})\check{d}_v^{(i)}}{\text{Var}(\tilde{d}_v^{(i)}) + \text{Var}(\check{d}_v^{(i)})} \right) \\ &= \frac{\text{Var}(\tilde{d}_v^{(i)})\text{Var}(\check{d}_v^{(i)})}{\text{Var}(\tilde{d}_v^{(i)}) + \text{Var}(\check{d}_v^{(i)})}, \quad i \in \{3, 10, 12, 13, 14\}. \end{aligned}$$

In the above derivation, the last equation holds because  $\tilde{d}_v^{(i)}$  and  $\check{d}_v^{(i)}$  are independent, which can be easily obtained from their definition in Eqs. (5), (6), (8), and (9).

For  $\text{Var}(\hat{d}_v^{(2)})$ , we have

$$\text{Var}(\hat{d}_v^{(2)}) = \text{Var}(\phi_v - \hat{d}_v^{(3)}) = \text{Var}(\hat{d}_v^{(3)}).$$

By the definition of  $\hat{d}_v^{(4)}$  and  $\hat{d}_v^{(7)}$ , we easily proof that the formulas

 <p>case 1: <math>u=u_1, w=u_2, r=v</math> case 2: <math>u=u_2, w=u_1, r=v</math></p>	 <p>case 1: <math>u=u_1, w=u_2, r=u_3</math></p>	 <p>case 1: <math>u=u_1, w=u_3, r=u_2</math> case 2: <math>u=u_2, w=u_3, r=u_1</math></p>
 <p>case 1: <math>u=u_1, w=u_2, r=u_3</math> case 2: <math>u=u_1, w=u_3, r=u_2</math></p>	 <p>case 1: <math>u=u_3, w=u_1, r=u_2</math></p>	 <p>case 1: <math>u=u_1, w=u_2, r=u_3</math> case 2: <math>u=u_1, w=u_3, r=u_2</math> case 3: <math>u=u_2, w=u_1, r=u_3</math> case 4: <math>u=u_2, w=u_3, r=u_1</math></p>
 <p>case 1: <math>u=u_1, w=u_3, r=u_2</math> case 2: <math>u=u_2, w=u_3, r=u_1</math></p>	 <p>case 1: <math>u=u_1, w=u_2, r=u_3</math> case 2: <math>u=u_1, w=u_3, r=u_2</math> case 3: <math>u=u_2, w=u_1, r=u_3</math></p>	<p>case 4: <math>u=u_2, w=u_3, r=u_1</math> case 5: <math>u=u_3, w=u_1, r=u_2</math> case 6: <math>u=u_3, w=u_2, r=u_1</math></p>

**Figure 9: The ways of Randgraf-4-3 sampling a CIS that includes  $v$  in different orbits. Numbers in blue are orbit IDs.  $u, w,$  and  $r$  in red are the variables in Algorithm 5.**

of their variances are

$$\begin{aligned} \text{Var}(\hat{d}_v^{(4)}) &= \sum_{j \in \{3, 8, 9, 10, 12, 13, 14\}} \chi_j^2 \text{Var}(\hat{d}_v^{(j)}) \\ &+ \sum_{j, k \in \{3, 8, 9, 10, 12, 13, 14\} \wedge j \neq l} \chi_j \chi_l \text{Cov}(\hat{d}_v^{(j)}, \hat{d}_v^{(l)}). \end{aligned}$$

$$\begin{aligned} \text{Var}(\hat{d}_v^{(7)}) &= \text{Var}(\hat{d}_v^{(11)}) + \text{Var}(\hat{d}_v^{(13)}) + \text{Var}(\hat{d}_v^{(14)}) \\ &+ \sum_{j, l \in \{11, 13, 14\} \wedge j \neq l} \text{Cov}(\hat{d}_v^{(j)}, \hat{d}_v^{(l)}), \end{aligned}$$

The covariances in the above formulas of  $\text{Var}(\hat{d}_v^{(4)})$  and  $\text{Var}(\hat{d}_v^{(7)})$  are computed as

1. When  $j, l \in \{5, 8, 11\}$  and  $i \neq l$ , by the definition of  $\hat{d}_v^{(j)}$  in Eq. (4) and Theorem 1, we have  $\text{Cov}(\hat{d}_v^{(j)}, \hat{d}_v^{(l)}) = -\frac{d_v^{(j)} d_v^{(l)}}{K^{(4,1)}}$ .

2. When  $j \in \{5, 8, 11\}$ , by the definition of  $\hat{d}_v^{(3)}$  and  $\hat{d}_v^{(j)}$  in Eqs. (7) and (4), we have

$$\begin{aligned} \text{Cov}(\hat{d}_v^{(3)}, \hat{d}_v^{(j)}) &= \text{Cov}(\lambda_v^{(3,1)} \tilde{d}_v^{(3)} + \lambda_v^{(3,2)} \tilde{d}_v^{(3)}, \hat{d}_v^{(j)}) \\ &= \lambda_v^{(3,1)} \text{Cov}(\tilde{d}_v^{(3)}, \hat{d}_v^{(j)}) + \lambda_v^{(3,2)} \text{Cov}(\tilde{d}_v^{(3)}, \hat{d}_v^{(j)}). \end{aligned}$$

Since  $\tilde{d}_v^{(3)}$  and  $\hat{d}_v^{(j)}$  are computed based independent samples generated by Randgraf-3-1 and Randgraf-4-1 respectively, we have  $\text{Cov}(\tilde{d}_v^{(3)}, \hat{d}_v^{(j)}) = 0$ . From Theorem 1, we have  $\text{Cov}(\tilde{d}_v^{(3)}, \hat{d}_v^{(j)}) = -\frac{d_v^{(3)} d_v^{(j)}}{K^{(4,1)}}$ . Therefore, we have  $\text{Cov}(\hat{d}_v^{(3)}, \hat{d}_v^{(j)}) = -\frac{\lambda_v^{(3,1)} d_v^{(3)} d_v^{(j)}}{K^{(4,1)}}$ .

3. When  $j, l \in \{6, 9\}$  and  $j \neq l$ , by the definition of  $\hat{d}_v^{(j)}$  in Eq. (4) and Theorem 1, we have  $\text{Cov}(\hat{d}_v^{(j)}, \hat{d}_v^{(l)}) = -\frac{d_v^{(j)} d_v^{(l)}}{K^{(4,2)}}$ .

4. When  $j, l \in \{10, 12, 13, 14\}$  and  $j \neq l$ , by the definition of  $\hat{d}_v^{(j)}$  in Eq. (10), we have  $\text{Cov}(\hat{d}_v^{(j)}, \hat{d}_v^{(l)}) = \text{Cov}(\lambda_v^{(j,1)} \tilde{d}_v^{(j)} + \lambda_v^{(j,2)} \tilde{d}_v^{(j)}, \lambda_v^{(l,1)} \tilde{d}_v^{(l)} + \lambda_v^{(l,2)} \tilde{d}_v^{(l)})$ . By the definitions of  $\tilde{d}_v^{(j)}$  and  $\tilde{d}_v^{(l)}$  in Eqs. (8) and (9), we find that  $\tilde{d}_v^{(j)}$  and  $\tilde{d}_v^{(l)}$  are independent, and  $\tilde{d}_v^{(j)}$  and  $\tilde{d}_v^{(l)}$  are independent. Moreover, from Theorem 1, we have  $\text{Cov}(\tilde{d}_v^{(j)}, \tilde{d}_v^{(l)}) = -\frac{d_v^{(j)} d_v^{(l)}}{K^{(4,1)}}$  and  $\text{Cov}(\tilde{d}_v^{(j)}, \tilde{d}_v^{(l)}) = -\frac{d_v^{(j)} d_v^{(l)}}{K^{(4,2)}}$ .

Therefore, we have  $\text{Cov}(\hat{d}_v^{(j)}, \hat{d}_v^{(l)}) = -\sum_{k=1,2} \frac{\lambda_v^{(j,k)} \lambda_v^{(l,k)} d_v^{(j)} d_v^{(l)}}{K^{(4,k)}}$ .

5. When  $j \in \{3, 5, 8, 11\}$  and  $l \in \{6, 9\}$ ,  $\hat{d}_v^{(j)}$  and  $\hat{d}_v^{(l)}$  are independent because  $\hat{d}_v^{(j)}$  are computed based on samples generated by

Randgraf-3-1 and Randgraf-4-1, while  $\hat{d}_v^{(l)}$  are computed based on samples generated by Randgraf-4-2.

6. When  $j \in \{5, 8, 11\}$  and  $l \in \{10, 12, 13, 14\}$ , we have  $\text{Cov}(\hat{d}_v^{(j)}, \hat{d}_v^{(l)}) = \text{Cov}(\hat{d}_v^{(j)}, \lambda_v^{(l,1)} \tilde{d}_v^{(l)} + \lambda_v^{(l,2)} \tilde{d}_v^{(l)})$  by the definition of  $\hat{d}_v^{(j)}$  in Eq. (10). By the definition of  $\hat{d}_v^{(j)}$  and  $\tilde{d}_v^{(l)}$  in Eqs. (4) and (9), we find that  $\hat{d}_v^{(j)}$  and  $\tilde{d}_v^{(l)}$  are independent. Moreover, by Theorem 1 and the definition of  $\hat{d}_v^{(j)}$  and  $\tilde{d}_v^{(l)}$  in Eqs. (4) and (8), we have  $\text{Cov}(\hat{d}_v^{(j)}, \tilde{d}_v^{(l)}) = -\frac{d_v^{(j)} d_v^{(l)}}{K^{(4,1)}}$ . Therefore, we have  $\text{Cov}(\hat{d}_v^{(j)}, \hat{d}_v^{(l)}) = -\frac{\lambda_v^{(l,1)} d_v^{(j)} d_v^{(l)}}{K^{(4,1)}}$ .

7. When  $j \in \{6, 9\}$  and  $l \in \{10, 12, 13, 14\}$ , by the definition of  $\hat{d}_v^{(j)}$  in Eq. (10), we have  $\text{Cov}(\hat{d}_v^{(j)}, \hat{d}_v^{(l)}) = \text{Cov}(\hat{d}_v^{(j)}, \lambda_v^{(l,1)} \tilde{d}_v^{(l)} + \lambda_v^{(l,2)} \tilde{d}_v^{(l)})$ . By the definition of  $\hat{d}_v^{(j)}$  and  $\tilde{d}_v^{(l)}$  in Eqs. (4) and (8), we find that  $\hat{d}_v^{(j)}$  and  $\tilde{d}_v^{(l)}$  are independent. Moreover, by Theorem 1 and the definition of  $\hat{d}_v^{(j)}$  and  $\tilde{d}_v^{(l)}$  in Eqs. (4) and (8), we have  $\text{Cov}(\hat{d}_v^{(j)}, \tilde{d}_v^{(l)}) = -\frac{d_v^{(j)} d_v^{(l)}}{K^{(4,2)}}$ . Therefore, we have  $\text{Cov}(\hat{d}_v^{(j)}, \hat{d}_v^{(l)}) = -\frac{\lambda_v^{(l,2)} d_v^{(j)} d_v^{(l)}}{K^{(4,2)}}$ .

8. When  $j \in \{10, 12, 13, 14\}$ , by the definition of  $\hat{d}_v^{(3)}$  and  $\hat{d}_v^{(j)}$  in Eqs. (7) and (10), we have  $\text{Cov}(\hat{d}_v^{(j)}, \hat{d}_v^{(3)}) = \text{Cov}(\lambda_v^{(j,1)} \tilde{d}_v^{(j)} + \lambda_v^{(j,2)} \tilde{d}_v^{(j)}, \lambda_v^{(3,1)} \tilde{d}_v^{(3)} + \lambda_v^{(3,2)} \tilde{d}_v^{(3)})$ . By the definition of  $\tilde{d}_v^{(3)}$ ,  $\tilde{d}_v^{(j)}$ ,  $\tilde{d}_v^{(j)}$ , and  $\tilde{d}_v^{(3)}$  in Eqs. (5), (6), (8), and (9), we find that  $\tilde{d}_v^{(3)}$  and  $\tilde{d}_v^{(j)}$  are independent,  $\tilde{d}_v^{(3)}$  and  $\tilde{d}_v^{(j)}$  are independent, and  $\tilde{d}_v^{(3)}$  and  $\tilde{d}_v^{(j)}$  are independent. We also have  $\text{Cov}(\tilde{d}_v^{(3)}, \tilde{d}_v^{(j)}) = -\frac{d_v^{(3)} d_v^{(j)}}{K^{(4,1)}}$  from Theorem 1. Thus, we have  $\text{Cov}(\hat{d}_v^{(j)}, \hat{d}_v^{(3)}) = -\frac{\lambda_v^{(3,1)} \lambda_v^{(j,1)} d_v^{(3)} d_v^{(j)}}{K^{(4,1)}}$ .

## 10. REFERENCES

- [1] Natasa Przulj. Biological network comparison using graphlet degree distribution. *Bioinformatics*, 23(2):177–183, 2007.
- [2] Tijana Milenkovic and Natasa Przulj. Uncovering biological network function via graphlet degree signatures. *Cancer Informatics*, 6:257–273, 2008.
- [3] Tijana Milenkovic, Vesna Memisevic, Anand K. Ganesan, and Natasa Przulj. Systems-level cancer gene identification from protein interaction network topology applied to melanogenesis-related functional genomics data. *Journal of The Royal Society Interface*, 7(44):423–437, 2010.
- [4] Jihang Ye, Hong Cheng, Zhe Zhu, and Minghua Chen. Predicting positive and negative links in signed social

- networks by transfer learning. In *22nd International World Wide Web Conference, WWW '13, Rio de Janeiro, Brazil, May 13-17, 2013*, pages 1477–1488, 2013.
- [5] Meng Fang, Jie Yin, Xingquan Zhu, and Chengqi Zhang. Trgraph: Cross-network transfer learning via common signature subgraphs. *IEEE Trans. Knowl. Data Eng.*, 27(9):2536–2549, 2015.
- [6] Bifan Wei, Jun Liu, Jian Ma, Qinghua Zheng, Wei Zhang, and Boqin Feng. Motif-based hyponym relation extraction from wikipedia hyperlinks. *IEEE Trans. Knowl. Data Eng.*, 26(10):2507–2519, 2014.
- [7] Charalampos E. Tsourakakis, U Kang, Gary L. Miller, and Christos Faloutsos. Doulion: Counting triangles in massive graphs with a coin. In *Proceedings of ACM KDD*, 2009.
- [8] A.Pavany, Kanat Tangwongsan, Srikanta Tirthapuraz, and Kun-Lung Wu. Counting and sampling triangles from a graph stream. In *Proceedings of VLDB*, pages 1870–1881, 2013.
- [9] Madhav Jha, C. Seshadhri, and Ali Pinar. A space efficient streaming algorithm for triangle counting using the birthday paradox. In *Proceedings of ACM SIGKDD*, pages 589–597, 2013.
- [10] N.K. Ahmed, N. Duffield, J. Neville, and R. Kompella. Graph sample and hold: A framework for big-graph analytics. In *Proceedings of ACM SIGKDD*, pages 589–597, 2014.
- [11] Madhav Jha, C. Seshadhri, and Ali Pinar. Path sampling: A fast and provable method for estimating 4-vertex subgraph counts. In *Proceedings of WWW*, pages 495–505, 2015.
- [12] Jure Leskovec, Daniel Huttenlocher, and Jon Kleinberg. Predicting positive and negative links in online social networks. In *Proceedings of WWW*, pages 641–650, April 2010.
- [13] Franklin A. Graybill and R. B. Deal. Combining unbiased estimators. *Biometrics*, 15(4):543–550, dec 1959.
- [14] Alan Mislove, Massimiliano Marcon, Krishna P. Gummadi, Peter Druschel, and Bobby Bhattacharjee. Measurement and analysis of online social networks. In *Proceedings of ACM SIGCOMM IMC*, pages 29–42, October 2007.
- [15] Lubos Takac and Michal Zabovsky. Data analysis in public social networks. In *International Scientific Conference and International Workshop Present Day Trends of Innovations*, pages 1–6, May 2012.
- [16] Google programming contest. <http://www.google.com/programming-contest/>, 2002.
- [17] Ethan R. Elenberg, Karthikeyan Shanmugam, Michael Borokhovich, and Alexandros G. Dimakis. Distributed estimation of graph 4-profiles. In *Proceedings of WWW*, April 2016.
- [18] Noga Alon, Raphael Yuster, and Uri Zwick. Color-coding. *J. ACM*, 42(4):844–856, July 1995.
- [19] Nadav Kashtan, Shalev Itzkovitz, Ron Milo, and Uri Alon. Efficient sampling algorithm for estimating subgraph concentrations and detecting network motifs. *Bioinformatics*, 20(11):1746–1758, 2004.
- [20] Sebastian Wernicke. Efficient detection of network motifs. *IEEE/ACM Transactions on Computational Biology and Bioinformatics*, 3(4):347–359, 2006.
- [21] Saeed Omid, Falk Schreiber, and Ali Masoudi-nejad. Moda: An efficient algorithm for network motif discovery in biological networks. *Genes and Genet systems*, 84(5):385–395, 2009.
- [22] Mansurul A Bhuiyan, Mahmudur Rahman, Mahmuda Rahman, and Mohammad Al Hasan. Guise: Uniform sampling of graphlets for large graph analysis. In *Proceedings of IEEE ICDM*, pages 91–100, December 2012.
- [23] Mahmudur Rahman, Mansurul Bhuiyan, and Mohammad Al Hasan. Graft: An approximate graphlet counting algorithm for large graph analysis. In *Proceedings of ACM CIKM*, 2012.
- [24] Pinghui Wang, John C.S. Lui, Junzhou Zhao, Bruno Ribeiro, Don Towsley, and Xiaohong Guan. Efficiently estimating motif statistics of large networks. *ACM Transactions on Knowledge Discovery from Data*, 2014.
- [25] Pinghui Wang, John C. S. Lui, and Don Towsley. Minfer: Inferring motif statistics from sampled edges. *CoRR*, abs/1502.06671, 2015.
- [26] Pinghui Wang, Jing Tao, Junzhou Zhao, and Xiaohong Guan. Moss: A scalable tool for efficiently sampling and counting 4- and 5-node graphlets. *CoRR*, abs/1509.08089, 2015.